4 Resultados

4.1. Bloque 1

En este bloque de resultados se presentan los estudios realizados sobre los canales de potasio dependientes de voltaje presentes en macrófagos y su regulación ante distintos estímulos de proliferación y activación celular.

En concreto, en la primera contribución que se adjunta se describe cómo los canales de potasio Kv1.3, Kv1.5 y Kir2.1 son los responsables de las corrientes de salida dependiente de voltaje y de rectificación de entrada que se detectan en estas células. En este trabajo se muestra cómo Kv1.3 y Kir2.1 están altamente regulados tanto por el factor de crecimiento MCSF, como por factores inductores de la activación de los macrófagos como son el lipopolisacárido y la citoquina TNFα. Los estudios de electrofisiología realizados sugieren que el complejo funcional generador de la corriente de salida de potasio podría diferir entre macrófagos proliferantes y activados aunque Kv1.3 seguiría siendo la principal entidad molecular responsable de esta corriente. Por último, estos estudios muestran cómo, no sólo Kv1.3 se ve regulado en los procesos de proliferación y activación, sino que se requiere su participación en estos procesos.

La segunda contribución que se adjunta en este bloque muestra cómo la regulación de estos canales por LPS y TNFα, no se restringe únicamente a los macrófagos, sino que esta modulación es un mecanismo general que puede ser importante en diferentes patologías sistémicas en las que estos mediadores estén presentes como caquexia, sepsis o inflamación crónica.

CONTRIBUCIONES

4.1.1. Differential voltage-dependent K$^+$ channel responses during proliferation and activation in macrophages.

4.1.2. The systemic inflammatory response is involved in the regulation of K$^+$ channel expression in brain via TNF-α-dependent and -independent pathways.

Differential Voltage-dependent K+ Channel Responses during Proliferation and Activation in Macrophages*

Rubén Vicente,[a,b,c] Artur Escalada,[b,d,e] Mireia Coma,[a] Gemma Fuster,[a] Ester Sánchez-Tilló,[f] Carmen López-Iglesias,[g] Concepció Soler,[h,i] Carles Solsona,[d,j] Antonio Celada,[f,k] and Antonio Felipe[a,l]

From the [a]Molecular Physiology Laboratory, Departament de Bioquímica i Biologia Molecular, [g]Unitat de Reconeixement Molecular in Situ, Serveis Cientificotècnics, [f]Macrophage Biology Group, Biomedical Research Institute of Barcelona, [h]Departament de Fisiologia, Universitat de Barcelona, E-08028 Barcelona, Spain and the [d]Cellular and Molecular Neurobiology Laboratory, Departament de Biologia Cellular i Anatomia Patològica, Universitat de Barcelona-Campus de Bellvitge, E-08907 Hospitalet de Llobregat, Spain

Voltage-dependent K+ channels (VDPC) are expressed in most mammalian cells and involved in the proliferation and activation of lymphocytes. However, the role of VDPC in macrophage responses is not well established. This study was undertaken to characterize VDPC in macrophages and determine their physiological role during proliferation and activation. Macrophages proliferate until an endotoxic shock halts cell growth and they become activated. By inducing a schedule that is similar to the physiological pattern, we have identified the VDPC in non-transformed bone marrow-derived macrophages and studied their regulation. Patch clamp studies demonstrated that cells expressed outward delayed and inwardly rectifying K+ currents. Pharmacological data, mRNA, and protein analysis suggest that these currents were mainly mediated by Kv1.3 and Kir2.1 channels. Macrophage colony-stimulating factor-dependent proliferation induced both channels. Lipopolysaccharide (LPS)-induced activation differentially regulated VDPC expression. While Kv1.3 was further induced, Kir2.1 was down-regulated. TNF-α mimicked LPS effects, and studies with TNF-α receptor I/II double knockout mice demonstrated that LPS regulation mediates such expression by TNF-α-dependent and -independent mechanisms. This modulation was dependent on mRNA and protein synthesis. In addition, bone marrow-derived macrophages expressed Kv1.5 mRNA with no apparent regulation. VDPC activities seem to play a critical role during proliferation and activation because not only cell growth, but also inducible nitric-oxide synthase expression were inhibited by blocking their activities. Taken together, our results demonstrate that the differential regulation of VDPC is crucial in intracellular signals determining the specific macrophage response.

Immune system responses to an antigen involve a complex network of several cell types. Among them, the mononuclear phagocyte family comprises numerous cell types, including tissue macrophages, Kupffer cells, dermal Langerhans cells, osteoclasts, microglia, and perhaps some of the interdigitating and follicular dendritic cells from lymphoid organs (1). Macrophages perform critical functions in the immune system, acting as regulators of homeostasis and as effector cells in infection, wounding, and tumor growth. In response to different growth factors and cytokines, macrophages can proliferate, become activated or differentiate. As monocytes differentiate into mature, non-proliferating macrophages they can produce a large variety of responses, including chemotaxis, phagocytosis, and secretion of numerous cytokines and other substances. To elicit the appropriate physiological response plasma membrane protein expression changes dramatically from proliferation to activation (2).

Voltage-dependent potassium channels (VDPC)[1] are a group of plasma membrane ion channels with a key role in controlling repolarization and resting membrane potential in electrically excitable cells. K+ channels are also involved in the maintenance of vascular smooth muscle tone, glucose-stimulated insulin release by β-pancreatic cells, cell volume regulation, and cell growth (3). Leukocytes express a number of voltage-gated and/or second messenger-modulated ion channels, and the electrophysiological properties of many of these channels are known (4–17). Despite considerable progress, important questions remain unsolved, the relationship of these proteins to cell function being one of the most relevant (18–20). VDPC are associated with macrophage functions such as migration, proliferation, activation, and cytokine production (see Refs. 18 and 19 for reviews). Although microglia appears to express most neuronal channels, circulating macrophages have a number of VDPC yet to be defined (19). These proteins have been studied

[1] The abbreviations used are: VDPC, voltage-dependent potassium channels; BMDM, bone marrow-derived macrophages; iNOS, inducible nitric-oxide synthase; LPS, lipopolysaccharide; M-CSF, macrophage-colony stimulating factor; MgTx, rMargatoxin; TNF-α, tumor necrosis factor α; IL, interleukin; RT, reverse transcriptase; PBS, phosphate-buffered saline; ANOVA, analysis of variance.
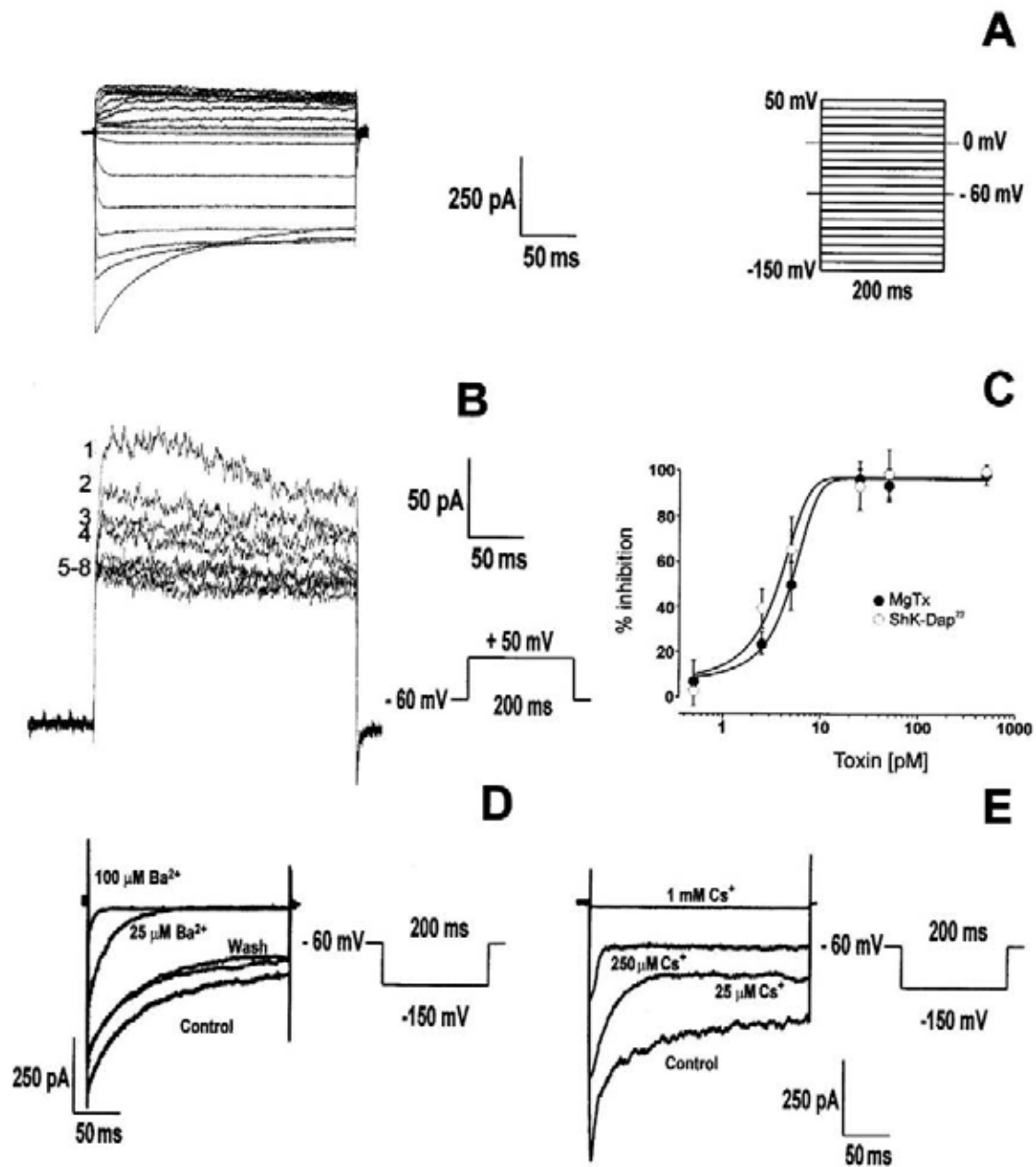
81

46308   *Differential K⁺ Channel Regulation in Macrophages*

FIG. 1. **Macrophages express outward delayed and inwardly rectifying K⁺ currents.** *A*, representative traces of K⁺ currents. Cells were held at −60 mV and pulse potentials were applied as indicated. *B*, cumulative inactivation of outward currents. Currents were elicited by a train of 8 depolarizing voltage steps (200 ms duration) to +50 mV once every 400 ms. The current amplitude became progressively smaller from the first trace to the last. *C*, dose-dependent inhibition curves of the outward current by MgTx (●) and ShK-Dap[22] (○). Currents were evoked at +50 mV from a holding potential of −60 mV during a pulse potential of 200 ms. The percent of inhibition was calculated by comparing the current at a given concentration of toxin *versus* that obtained in its absence. *D*, dose-dependent inhibition of the inwardly rectifying current by Ba²⁺. *E*, dose-dependent inhibition of the inwardly rectifying current by Cs⁺.

in various cellular models, and outward delayed and inwardly rectifying K⁺ currents have been identified. Furthermore, the presence of the *shaker*-like Kv1.3 and Kir2.1 channels has been detected in some studies. However, the use of either activated or transformed macrophage cell lines has led to controversial results (4–20). Thus, while a high-conductance Ca²⁺-depend-

ent K⁺ channel has been clearly identified as an early step in transmembrane signal transduction in macrophages (21), the physiological role of VDPC in either proliferation or activation is not known. Primary culture of bone marrow-derived macrophages (BMDM) is a unique non-transformed model in which proliferation and activation can be studied separately, mimick-

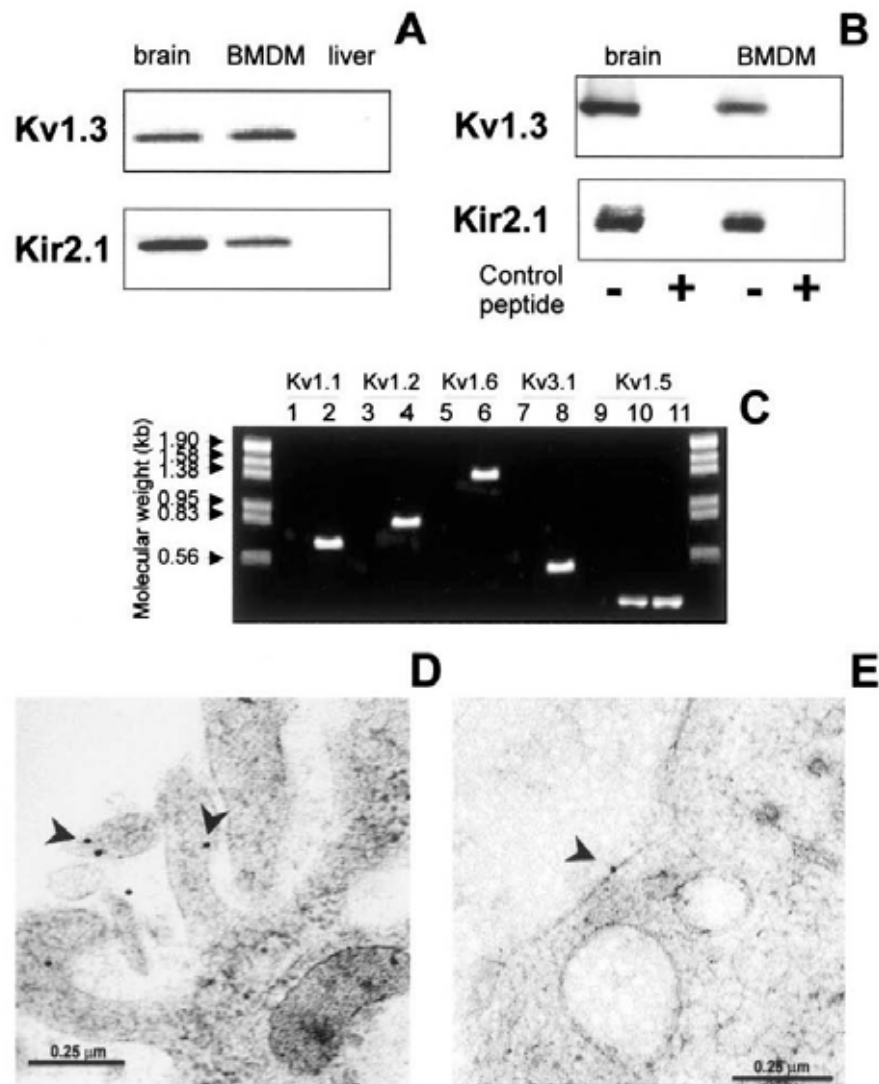*Differential K⁺ Channel Regulation in Macrophages*   46309

Fig. 2. **Voltage-dependent K⁺ channel expression in macrophages.** *A*, mRNA expression of Kv1.3 and Kir2.1 in the mouse brain and macrophages but not in the liver. 1 μg of total RNA was used in RT-PCR reactions as described under "Experimental Procedures." *B*, Kv1.3 and Kir2.1 protein expression in the mouse brain and BMDM. Western blot analysis were performed in the presence and the absence of the control antigen peptide. *C*, VDPC expression in BMDM. RT-PCR was set as described under "Experimental Procedures" with oligonucleotides from Kv1.1 (accession number NM_010595; base pairs 1102–1807), Kv1.2 (accession number NM_008417, base pairs 841–1691), Kv1.5 (accession number AF302768, base pairs 3003–3337), Kv1.6 (accession number NM_013568, base pairs 233–1822), and Kv3.1 (accession number Y07521, base pairs 727–1231). *Lanes 1, 3, 5, 7, 9,* and *10,* PCR reactions from BMDM. *Lanes 2, 4, 6, 8, 11,* PCR from mouse brain. *Lane 9* of Kv1.5 is a negative control in the absence of the RT reaction. PCR products were run in a 1% agarose gel. *D* and *E,* immunocytochemical electron microscopic detection of Kv1.3 and Kir2.1 proteins, respectively. *Arrows* show specific channel protein localization. *Bars* indicate 0.25-μm scale.

ing physiological processes that occur in the body (22). Macrophages are generated in the bone marrow and, through the bloodstream, reach all tissues, stop proliferation and become activated (2). Macrophage colony-stimulating factor (M-CSF) is the specific growth factor for this cell type (23). On the other hand, lipopolysaccharide (LPS) is a major component of the outer Gram-negative bacteria membrane, which interacts with monocytes/macrophages and induces a variety of intracellular signaling cascades, finally leading to the release of endogenous mediators such as TNF-α, IL-1, and IL-6 (24). Furthermore, LPS triggers cellular activation and apoptosis by an early TNF-α-dependent mechanism (25).

Several VDPC candidates could be present in macrophages and our first interest was to identify these channels in a primary culture of BMDM. Macrophages mainly expressed the outward delayed Kv1.3 and the inwardly rectifying Kir2.1 potassium channels. Because VDPC could be involved not only in proliferation but also in activation, our second goal was to determine their specific role by inducing a schedule that is similar to the physiological pattern in BMDM. M-CSF-dependent proliferation led to an up-regulation of VDPC generating an increase in potassium current densities without changes in current kinetics. When cells were further incubated with LPS the electrophysiological properties changed dramatically.

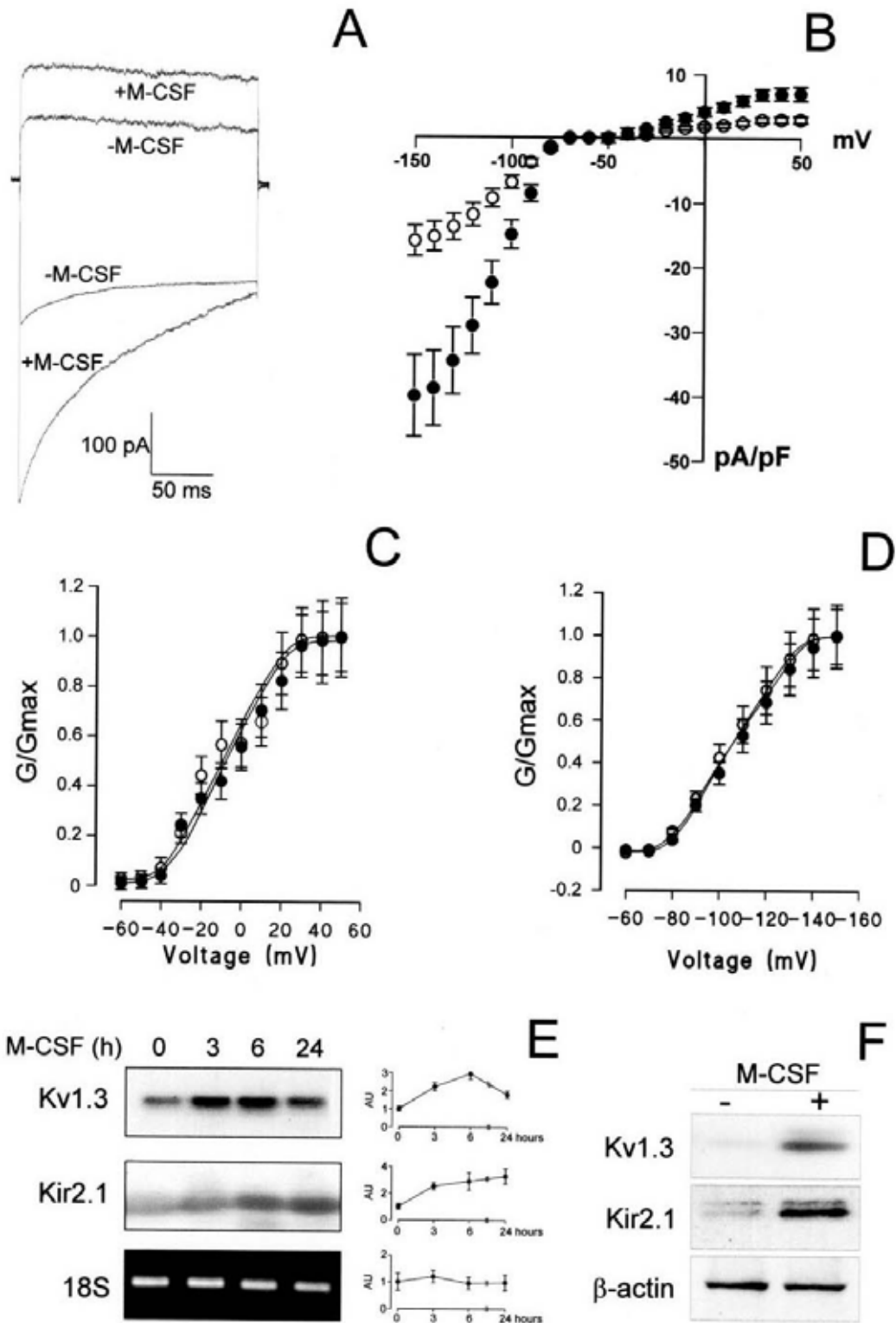FIG. 3. **M-CSF-dependent proliferation induces VDPC in macrophages.** *A*, cells were incubated for 24 h in the presence (*+M-CSF*) or absence (*–M-CSF*) of the growth factor. Representative outward and inward traces were elicited by a hyperpolarizing step from −60 to −150 mV and a depolarizing step from −60 to +50 mV for 200 ms, respectively. *B*, current density *versus* voltage relationship of K⁺ currents. Macrophages

Differential K⁺ Channel Regulation in Macrophages   46311

Thus, Kv1.3 was further increased, whereas Kir2.1 was down-regulated. We also show that TNF-α partially mimicked the response to LPS, suggesting that there are TNF-α-dependent and -independent mechanisms mediating LPS-induced VDPC modulation in macrophages. Our results have physiological relevance and indicate that VDPC expression is important as an early regulatory step, and fine-tuning modulation of their expression is crucial to the specific membrane signaling that triggers the appropriate immune response.

EXPERIMENTAL PROCEDURES

Animals and Cell Culture—BMDM from 6- to 10-week-old BALB/c or C57/BL6 mice (Charles River Laboratories) were used. Cells were isolated and cultured as described elsewhere (22). Briefly, animals were killed by cervical dislocation, and both femurs were dissected removing adherent tissue. The ends of bones were cut off and the marrow tissue was flushed by irrigation with medium. The marrow plugs were passed through a 25-gauge needle for dispersion. The cells were cultured in plastic dishes (150 mm) in Dulbecco's modified Eagle's medium containing 20% fetal bovine serum and 30% supernatant of L-929 fibroblast (L-cell) conditioned media as a source of M-CSF. Macrophages were obtained as a homogeneous population of adherent cells after 7 days of culture and maintained at 37 °C in a humidified 5% CO$_2$ atmosphere. For experiments, they were cultured with the same tissue culture differentiation medium (Dulbecco's modified Eagle's medium, 20% fetal bovine serum, 30% L-cell medium) or arrested at G$_0$ by M-CSF deprivation in Dulbecco's modified Eagle's medium supplemented with 10% fetal bovine serum for at least 18 h. G$_0$-arrested cells were further incubated in the absence or presence of recombinant murine M-CSF (1200 units/ml), with or without LPS (100 ng/ml) or TNF-α (100 ng/ml), for the indicated times. In some experiments, cells were exposed to rMargatoxin (MgTx), BaCl$_2$, cycloheximide, and actinomycin D as previously described (26–30).

The TNF-α receptor I/II double knockout mice (C57/BL6) used in this study were generated and characterized as previously reported (25, 31). All animal handling was approved by the ethics committee of the University of Barcelona in accordance with EU regulations.

DNA Synthesis—DNA synthesis was measured as the incorporation of [³H]thymidine (Amersham Biosciences) to DNA, as described elsewhere (22). Briefly, macrophages (5×10^4) were seeded in 24-well plates in 1 ml of medium without M-CSF for at least 18 h. Cells were then cultured for a further 24 h in the absence or presence of M-CSF with/without LPS, TNF-α, MgTx, or BaCl$_2$ (1 mM). Finally, the medium was removed and replaced with 0.5 ml of the same medium containing 1 μCi/ml [³H]thymidine. After three additional hours of incubation, cells were fixed in 70% methanol, washed three times in ice-cold 10% trichloroacetic acid, and solubilized in 1% SDS and 0.3% NaOH. The whole content of the well was used for counting radioactivity.

RNA Isolation and RT-PCR Analysis—Total RNA from mouse macrophages, brain, and liver was isolated using the Tripure reagent (Roche Diagnostics), following the manufacturer's instructions. Samples were further treated with the DNA-free kit from Ambion Inc. to remove DNA.

Ready-to-Go RT-PCR beads (Amersham Biosciences) were used in a one-step RT-PCR as described elsewhere (22, 32–34). Total RNA and selected primers at 1 μM were added to the beads. The RT reaction was initiated by incubating the mixture at 42 °C for 30 min. Once the first-strand cDNA had been synthesized, the conditions were set for further PCR: 92 °C for 30 s, either 55 °C (Kv1.3 and 18S) or 60 °C (Kir2.1) for 1 min and 72 °C for 2 min. These settings were applied for 40 cycles. Every 10 cycles, 10 μl of the total reaction was collected in a separate tube for further electrophoresis and analysis. A range of dilutions of RNA from each independent sample was performed to obtain an exponential phase of amplicon production (not shown) as described previously (32). The same independent RNA aliquot was used to analyze the VDPC mRNA expression and the respective amount of 18 S rRNA. Primer sequences and accession numbers were: Kv1.3 (accession

number M30441), forward, 5′-CTCATCTCCATTGTCATCTTCTGA-3′ (base pairs 741–765) and reverse, 5′-TTGAATTGGAAACAATCAC-3′ (base pairs 1459–1440); Kir2.1 (accession number AF021136), forward, 5′-TGGCTGTGTGTTTTGGTTGATAGC-3′ (base pairs 297–320) and reverse, 5′-CTTTGCCATCTTCGCCATGACTGC-3′ (base pairs 555–532); and 18 S (accession number X00686), forward, 5′-CGCAGAATTCCCA-CTCCCGACCC-3′ (base pairs 482–498) and reverse, 5′-CCCAAGCTC-CAACTACGAGC-3′ (base pairs 694–675). Kv1.5 and other Kv mRNA expression was analyzed by PCR as previously described (33). In all cases negative controls were performed in the absence of the RT reaction.

Once the exponential phase of the amplicon production had been determined the specificity of each product was confirmed in test RT-PCR using the appropriate cDNA probe in a Southern blot analysis. PCR-generated VDPC cDNA probes from mouse brain were subcloned using the pSTBlue-1 acceptor vector kit (Novagen) and the sequences were confirmed using the Big Dye Terminator Cycle sequencing kit and an ABI 377 sequencer (Applied Biosystems). EcoRI-digested [α-³²P]CTP random primer-labeled cDNAs were used as probes as previously described (34). At least three different filters were made from independent samples and representative blots are shown. Results were analyzed with Phoretix software (Nonlinear Dynamics).

Protein Extracts and Western Blot—Cells were washed twice in cold phosphate-buffered saline (PBS) and lysed on ice with lysis solution (1% Nonidet P-40, 10% glycerol, 50 mmol/liter HEPES, pH 7.5, 150 mmol/liter NaCl) supplemented with 1 μg/ml aprotinin, 1 μg/ml leupeptin, 86 μg/ml iodoacetamide, and 1 mM phenylmethylsulfonyl fluoride as protease inhibitors. Sample protein concentration was determined by Bio-Rad protein assay. The proteins from cell lysates (100 μg) were boiled at 95 °C in Laemmli SDS-loading buffer and separated on 10% SDS-PAGE. They were transferred to nitrocellulose membranes (Immobilon-P, Millipore), and blocked in 5% dry milk-supplemented 0.2% Tween 20 PBS prior to immunoreaction. To monitor Kv1.3 and Kir2.1 expression, rabbit polyclonal antibodies (Alomone Labs) were used. To study the expression of inducible nitric-oxide synthase (iNOS), a rabbit antibody against mouse iNOS (Santa Cruz Biotechnology) was used. The rabbit polyclonal anti-Kv1.5 antibody was a kind gift from Dr. M. M. Tamkun (Colorado State University). As a loading and transfer control, a monoclonal anti-β-actin antibody (Sigma) was used.

Electron Microscopy—Cell monolayers on Petri dishes were scraped and collected into PBS buffer. BMDM were cryofixed by high-pressure freezing using an EMPact (Leica). Freeze substitution was performed in an "Automatic Freeze Substitution system" (AFS) from Leica, using acetone containing 0.5% of uranyl acetate, for 3 days at −90 °C. On the fourth day, the temperature was slowly increased, 5 °C/h, to −50 °C. At this temperature samples were rinsed in acetone and then infiltrated and embedded in Lowicryl HM20. Ultrathin sections were picked up on Formvar-coated copper-palladium grids. For immunogold localization, samples were blocked with 10% fetal calf serum in PBS for 20 min and incubated at room temperature for 1 h with polyclonal anti-Kv1.3 or anti-Kir2.1 (1:200). Washes were performed with PBS prior to adding goat anti-rabbit conjugated to 10 nm colloidal gold (BioCell Research Laboratory) for 1 h at room temperature. Finally, samples were washed and contrasted with 2% uranyl acetate for 30 min and observed in a Hitachi 600AB electron microscope.

Electrophysiological Recordings—Whole cell currents were measured using the patch clamp technique. An EPC-9 (HEKA) with the appropriate software was used for data recording and analysis. Currents were filtered at 2.9 kHz. Series resistance compensation was always above 70%. Patch electrodes of 2–4 Mohms were fabricated in a P-97 puller (Sutter Instruments Co.) from borosilicate glass (outer diameter 1.2 mm and inner diameter 0.94 mm; Clark Electromedical Instruments Co.). Electrodes were filled with the following solution (in mM): 120 KCl, 1 CaCl$_2$, 2 MgCl$_2$, 10 HEPES, 11 EGTA, 20 D-glucose, adjusted to pH 7.3 with KOH. The extracellular solution contained (in mM): 120 NaCl, 5.4 KCl, 2 CaCl$_2$, 1 MgCl$_2$, 10 HEPES, 25 D-glucose, adjusted to pH 7.4 with NaOH. After establishing the whole cell configuration of the patch clamp technique macrophages were clamped to

were held at −60 mV and pulse potentials as described in the legend to Fig. 1 were applied. Conductance was plotted against test potentials. *C*, steady-state activation curves of the outward current. Conductance above holding potentials were normalized to the peak current density at +50 mV. *D*, steady-state activation curves of the inwardly rectifying current. Conductance below holding potentials were normalized to the current density at −150 mV. Symbols for *B–D panels* are: ○, −M-CSF; ●, +M-CSF. *E*, Kv1.3 and Kir2.1 mRNA expression. Samples were collected after the addition of M-CSF and RT-PCR analysis was performed as described under "Experimental Procedures" at the indicated times. Values are the mean ± S.E. ($n = 4$). Significant differences were found with Kv1.3 and Kir2.1 ($p < 0.001$, ANOVA). *F*, Kv1.3 and Kir2.1 protein expression in BMDM cultured during 24 h in the absence (−) or presence (+) of M-CSF.

46312   *Differential K⁺ Channel Regulation in Macrophages*

a holding potential of −60 mV. To evoke voltage-gated currents all cells were stimulated with 200-ms square pulses ranging from −150 to +50 mV in 10-mV steps. All recordings were routinely subtracted for leak currents.

The pharmacological characterization of the inward rectifier K⁺ current was performed by adding to the external solution $BaCl_2$ and CsCl at various concentrations (28). To block the outward current, MgTx and ShK-Dap²² were added to the external solution (26, 27). Before experiments, toxins were reconstituted to 10 μM in Tris buffer (0.1% bovine serum albumin, 100 mM NaCl, 10 mM Tris, pH 7.5). All recordings were done at room temperature (20–23 °C).

Reagents—Recombinant murine TNF-α was obtained from Prepo-Tech EC. Recombinant murine M-CSF was from R&D Systems. Cyclo-heximide, actinomycin D, LPS, CsCl, and $BaCl_2$ were purchased from Sigma, and MgTx from Alomone Labs. ShK-Dap²² was from Bachem Biosciences Inc. Other reagents were of analytical grade.

Analysis and Statistics—According to the solutions used, the calculated equilibrium potential for potassium was −79 mV (E_K) using the Nernst equation. The normalized G/G_{max} versus voltage curve was fitted using Boltzmann's equation: $G/G_{max} = 1/(1 + \exp^{((V_{1/2}-V)/k)})$, where $V_{1/2}$ is the voltage at which the current is half-activated and k is the slope factor of the activation curve.

Values are expressed as the mean ± S.E. The significance of differences was established by either Student's t test or one way ANOVA (Graph Pad, PRISM 3.0) for either two-group or two-factor comparison, respectively. A value of $p < 0.05$ was considered significant.

RESULTS

Macrophages Express Outward and Inward K⁺ Currents: Pharmacology and Molecular Characterization of Kv1.3 and Kir2.1—Cells ($n = 80$) plated in the presence in L-cell-conditioned medium expressed outward delayed and inward rectifier potassium currents (Fig. 1A). Following a train of 200-ms depolarizing pulses to +50 mV at 400-ms intervals, the outward current showed a characteristic cumulative inactivation phenomenon (Fig. 1B). Fig. 1C shows the effect of MgTx and ShK-Dap²² on the outward conductance. The IC_{50} for inhibition were ~5 and ~3 pM for MgTx and ShK-Dap²², respectively. These results indicated that Kv1.3 would be the main channel responsible for the outward potassium current. On the other hand, the high sensitivity to Ba^{2+} (Fig. 1D) and Cs^+ (Fig. 1E), together with the closed state above 0 mV of the inward current, indicated that the channel was Kir2.1. To identify K⁺ channels at the molecular level, we performed RT-PCR analyses. Mouse brain and liver RNAs were used as positive and negative controls, respectively. Fig. 2A shows that macrophages expressed Kv1.3 and Kir2.1 mRNA to a similar extent to that observed in the brain. In addition, specific Kv1.3 and Kir2.1 signals were obtained by Western blot analysis in brain and BMDM protein samples (Fig. 2B). The presence of other VDPC (Kv1.1, Kv1.2, Kv1.6, and Kv3.1) analyzed by RT-PCR was negative (Fig. 2C). However, BMDM expressed Kv1.5 mRNA but the protein expression was below detection levels analyzed by Western blot (Fig. 2C and data not shown).

The expression of Kv1.3 and Kir2.1 proteins in macrophages was further confirmed by electron microscopic immunocytochemical detection studies with specific antibodies (Fig. 2, D and E, respectively). Taken together, these data indicate that BMDM have outward delayed and inward rectifier potassium currents that are mainly conducted by Kv1.3 and Kir2.1 K⁺ channels.

M-CSF-dependent Proliferation Induces Kv1.3 and Kir2.1—M-CSF is the specific growth factor for this cell type. Macrophages incubated for about 18 h in the absence of this factor stopped cell growth (>98%) and became quiescent (22). The addition of M-CSF triggered macrophage proliferation (not shown) and outward and inward K⁺ currents were induced after 24 h of incubation (Fig. 3A). The current density (pA/pF)/voltage relationships depicted in Fig. 3B showed that M-CSF increased currents up to 3-fold. The number and density of the channels were increased during M-CSF-dependent prolifera-

tion. Whereas at +50 mV resting cells expressed ~30 channels/cell with a density of ~0.017 channel/μm^2, proliferating cells showed ~90 channels/cell and ~0.05 channel/μm^2. A large increase was also observed in the inward current at −150 mV. Thus, M-CSF-treated macrophages increased from ~80 to ~275 channels/cell and from ~0.044 to ~0.15 channel/μm^2 for the number and channel density, respectively. Normalized conductance demonstrated that both groups showed similar patterns. Thus, outward currents (Fig. 3C) indicated that channels were open at depolarizing potentials with a $V_{1/2}$ of −10.53 ± 2.8 and −11.33 ± 2.1 mV and k of 20 ± 3 and 21 ± 3 for resting (−M-CSF) and proliferating (+M-CSF) cells, respectively ($n = 20$). Moreover, the steady-state activation of inward currents (Fig. 3D) was also similar, with $V_{1/2}$ values of −105 ± 2 and −109 ± 2 mV and slopes k of −12.0 ± 1 and −12.4 ± 1 for −M-CSF and +M-CSF cells, respectively ($n = 20$).

Fig. 3E illustrates the time course of Kv1.3 and Kir2.1 gene expression after the addition of M-CSF. The expression of both VDPC increased by up to 3-fold. However, whereas Kv1.3 reached the highest levels after about 6 h, Kir2.1 expression increased steadily throughout the study. Similar changes were obtained in Kv1.3 and Kir2.1 protein abundance in BMDM incubated during 24 h in the presence of M-CSF (Fig. 3F). No differences were observed in the absence of M-CSF throughout the study. Taken together, these data indicate that M-CSF-dependent proliferation leads to long term increases in current densities of outward and inward currents in accordance with an induction in mRNA and protein expression.

LPS-induced Activation Regulates Differentially Kv1.3 and Kir2.1—Proliferating macrophages reach body tissues and are activated by physiological processes. The addition of LPS for 24 h in the presence of M-CSF inhibited proliferation (99.5 ± 0.5%, $n = 12$). LPS also increased the outward current concomitantly to a reduction in the inward current (Fig. 4A). The current density/voltage relationship depicted in Fig. 4B indicates that at depolarizing potentials the current was increased 4-fold, whereas at hyperpolarizing potentials the inward current was reduced about 5-fold. Thus, in the presence of LPS the number of the outward delayed rectifier functional channels and their density was 5 times larger that in its absence at +50 mV (~90 and ~420 channels/cell and ~0.05 and ~0.25 channel/μm^2, respectively). On the contrary, at −150 mV, the number and density of the inward channels decreased, being ~40 and ~275 channels/cell and ~0.022 and ~0.15 channel/μm^2 for LPS-treated and untreated macrophages, respectively. In the presence of 10 nM MgTx outward currents were totally inhibited, with no effect on the inward conductance (Fig. 4C). Fig. 4D shows the steady-state activation curves of the normalized outward current above the holding potential. Whereas $V_{1/2}$ values were similar for both groups (−12.8 ± 1.1 and −15.7 ± 3.6 mV for −LPS and +LPS, respectively, $n = 10$), k slope values were significantly different (21.0 ± 3 and 9.3 ± 1.2 for −LPS and +LPS, respectively, $p < 0.001, n = 10$). However, when the steady-state activation curves of inward currents were analyzed (Fig. 4E), both groups showed similar characteristics. Thus, $V_{1/2}$ values were −108 ± 2 and −105.8 ± 1 mV and k values were −12.6 ± 1 and −11.9 ± 1 for −LPS and +LPS, respectively ($n = 10$).

Fig. 5 shows Kv1.3 and Kir2.1 expression in the presence of M-CSF with or without LPS at different times. The presence of LPS induced the expression of Kv1.3 mRNA about 4-fold after 3 h (Fig. 5A). After 24 h, Kv1.3 mRNA still was ~275% above control. In contrast, Kir2.1 mRNA decreased steadily. Fig. 5B shows that the mRNA regulation observed for Kv1.3 and Kir2.1 was mirrored by similar changes in protein expression levels.
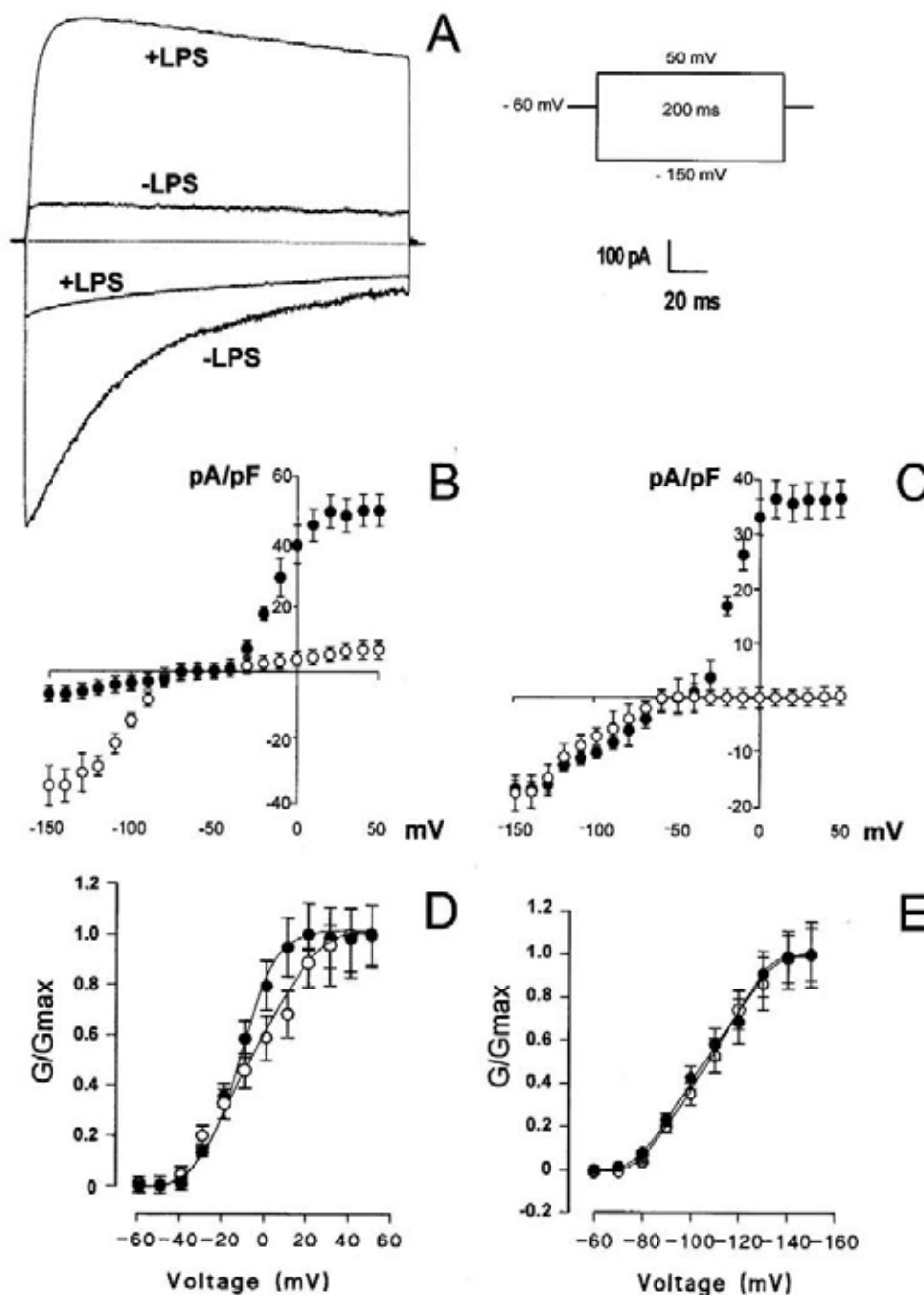
Fig. 4. **LPS-induced activation regulates K$^+$ currents differentially in macrophages.** BMDM were incubated with M-CSF for 24 h in the presence (+*LPS*) or absence (−*LPS*) of the endotoxin. *A*, representative outward and inward traces were elicited as indicated. *B*, current density *versus* voltage representation of K$^+$ currents. Macrophages were held at −60 mV and pulse potentials were applied as indicated in the legend to Fig. 1. *C*, current density/voltage relationship of the specific inhibition of outward K$^+$ currents by 10 nM MgTx. Cells were treated with LPS and currents were evoked in the presence (○) or absence (●) of MgTx. Pulse potentials were applied as indicated in the legend to Fig. 1. *D*, steady-state activation curve of the outward current. Conductance *above* the holding potentials were normalized to the peak current density at +50 mV. *E*, steady-state activation curves of the inwardly rectifying current. Conductance *below* the holding potentials were normalized to the peak current density at −150 mV. Symbols for *B–E* panels: ○, −LPS; ●, +LPS. Values are the mean ± S.E. (*n* = 10).

*TNF-α Regulates Kv1.3 and Kir2.1 Similarly to LPS, Evidence for LPS Modulation by TNF-α-dependent and -independent Mechanisms*—TNF-α produced by macrophages and

lymphocytes mediates a number of events induced by LPS, including activation, apoptosis, and the nucleoside uptake (25, 35). To examine whether TNF-α mediates LPS regulation of

46314   *Differential K⁺ Channel Regulation in Macrophages*

FIG. 5. LPS-induced activation up-regulates Kv1.3 and down-regulates Kir2.1 VDPC. *A*, RT-PCR analysis of Kv1.3 and Kir2.1 mRNA expression at different times after LPS treatment. Results from RT-PCR on 0.25 μg of total RNA for 30 cycles for Kv1.3 and Kir2.1 and 0.1 μg of RNA and 10 cycles for 18 S are shown. These conditions were at the exponential phase of the amplicon production as described under "Experimental Procedures." ●, Kv1.3; ○, Kir2.1; ■, 18 S. Significant differences were found with Kv1.3 and Kir2.1 ($p < 0.001$, ANOVA). *B*, Kv1.3 and Kir2.1 Western blot analysis. Cells were incubated for 24 h with (+*LPS*) or without (−*LPS*) the endotoxin. *Open bars*, Kv1.3; *closed bars*, Kir2.1; *hatched bars*, β-actin. **, $p < 0.01$; ***, $p < 0.001$ *versus* −LPS (Student's *t* test). Representative filters are shown. Values are mean ± S.E. of four independent experiments.
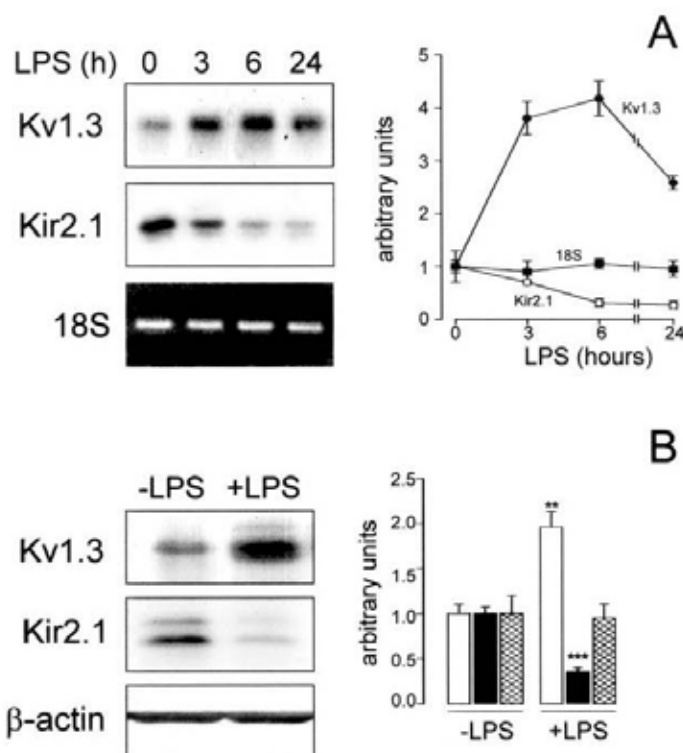
VDPC, macrophages in the presence of M-CSF were incubated for 24 h with (+TNF-α) or without (−TNF-α) TNF-α, and K⁺ currents were analyzed (Fig. 6). The cytokine increased the outward current and decreased the inward (Fig. 6A). Current density/voltage relationships (Fig. 6B) demonstrated that at depolarizing potentials the outward current was 3-fold induced while at hyperpolarizing potentials the inward was 6-fold lower. In addition, at a potential of +50 mV, there was a considerable increase in the number and density of outward channels (~90 and ~240 channels/cell; ~0.15 and ~0.22 channel/μm² for TNF-α untreated and treated cells, respectively), at −150 mV the number and density of the inward ones was lower (~275 and ~40 channels/cell; ~0.15 and ~0.022 channel/μm²). The steady-state activation curves for outward and inward currents are shown in Fig. 6, *C* and *D*, respectively. Outward current $V_{½}$ values were similar for both groups (−13.1 ± 2.7 and −17.0 ± 2.0 mV for −TNF-α and +TNF-α, respectively, $n = 9$). However, k slope values were different (21.0 ± 3 and 9.8 ± 1 for −TNF-α and +TNF-α, respectively, $p < 0.001$, $n = 9$). Inward currents were similar (Fig. 6D), with $V_{½}$ values −107.6 ± 2 and −107.9 ± 2 mV, and k values −16.7 ± 1.3 and −18.8 ± 1.5 for −TNF-α and +TNF-α, respectively ($n = 9$).

The expression of Kv1.3 and Kir2.1 mRNA and protein was also analyzed (Fig. 7). Kv1.3 mRNA induction peaked (~3-fold) after 3 h of incubation (Fig. 7A) and remained high throughout the study. Kir2.1 mRNA expression decreased for the first 6 h and remained low (about 30% of basal) for a further 24 h. Similarly to what was found with the mRNA, VDPC protein abundance was differentially regulated (Fig. 7B). Thus, whereas Kv1.3 showed a significant increase (~180%) after 24 h, Kir2.1 protein expression decreased about 50%.

To further explore the role of TNF-α in the LPS signaling, we used BMDM from TNF-α receptor I/II double knockout mice. As expected, TNF-α triggered Kv1.3 up-regulation and Kir2.1

down-regulation only in wild type (+/+) but not in TNF-α receptor I/II double knockout (−/−) cells (Fig. 8, *C* and *D*). Interestingly, LPS induced Kv1.3 and down-regulated Kir2.1 in both groups (Fig. 8, *A* and *B*). Taken together, these results indicate that although the autocrine production of TNF-α regulates VDPC similarly to LPS, redundant pathways must be involved.

Macrophage Proliferation and Activation Require VDPC Expression—Proliferation induced outward and inward K⁺ currents in macrophages. However, LPS and TNF-α triggered an induction of the outward current, whereas the inward current decreased (Fig. 9A). Concomitantly, the mRNA and protein expression of both VDPC were regulated differentially. Ion channels are under extensive regulation, and changes among different expression levels have been reported. However, in long term studies, VDPC mRNA mostly governs protein and activity (13, 34, 36). The regulation of K⁺ currents was dependent on mRNA and protein *de novo* synthesis because it was prevented by the presence of either actinomycin D or cycloheximide (Fig. 9A). To examine whether other VDPC, besides Kv1.3, were involved in the M-CSF-dependent proliferation and LPS- or TNF-α-induced activation, currents were evoked in the presence or absence of MgTx (Fig. 9B) and ShK-Dap²² (Fig. 9C). Similar results were obtained in all conditions, indicating that Kv1.3 is the main channel responsible for the outward currents. However, because Kv1.5 mRNA was detected in BMDM by RT-PCR, we analyzed its expression in macrophages cultured under distinct stimuli (Fig. 9D). Neither M-CSF-dependent proliferation nor LPS- and TNF-α-induced activation regulated Kv1.5 mRNA expression.

To further analyze the physiological role of VDPC during macrophage proliferation, cells were incubated for 24 h in the presence of M-CSF with or without MgTx and Ba²⁺. The addition of MgTx inhibited BMDM proliferation in a dose-dependent man-
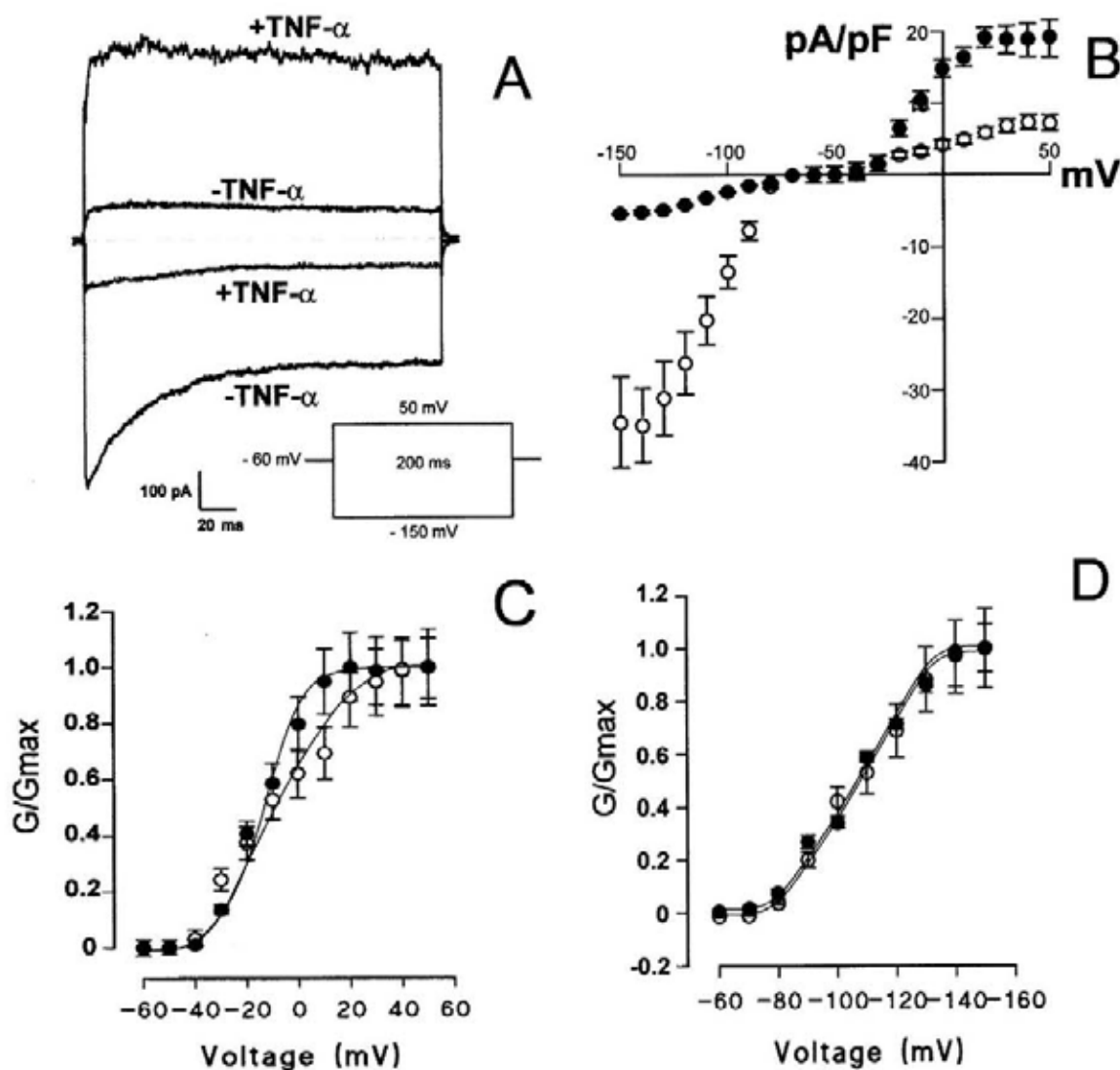
Differential K⁺ Channel Regulation in Macrophages   46315

FIG. 6. **TNF-α regulates K⁺ currents differentially in macrophages.** BMDM were incubated with M-CSF for 24 h in the presence (+*TNF-α*) or absence (−*TNF-α*) of the cytokine. A, representative outward and inward traces were elicited as indicated. B, current density/voltage relationship of K⁺ currents. Cells were held at −60 mV and pulse potentials were applied as indicated in the legend to Fig. 1. C, steady-state activation curves of the outward current. Conductance above holding potentials were normalized to the peak current at +50 mV. D, steady-state activation curves of the inwardly rectifying current. Conductance *below* the holding potentials were normalized to the peak current at −150 mV. ○, −TNF-α; ●, TNF-α. Values are the mean ± S.E. ($n = 9$).

ner with a IC_{50} of 2.2 nM (Fig. 9E). Moreover, cell growth was also lower in the presence of 1 mM Ba^{2+} (52 ± 6%, $n = 9$) and the addition of 10 nM MgTx further inhibited [³H]thymidine incorporation (69 ± 4%, $n = 6$, $p < 0.05$ *versus* 1 mM Ba^{2+} or 10 nM MgTx alone). These results indicate that Kv1.3 and Kir2.1 could be involved in the BMDM proliferation in an additive way.

The role of TNF-α in the LPS-induced activation seems to be partial, because not only the outward K⁺ current but also the proliferation were modulated to a lesser extent by TNF-α. Thus, while LPS totally abolished cell growth (see above), the inhibition of [³H]thymidine incorporation in the presence of TNF-α was 61 ± 5%. In addition, the pharmacological blockage of VDPC was additive, because proliferation was further decreased when either 10 nM MgTx or 1 mM Ba^{2+} was added to

TNF-α (91 ± 10 and 80 ± 4%, respectively, $n = 6$, $p < 0.001$ *versus* TNF-α alone).

The potential role of VDPC during proliferation and activation was further supported by the effects of MgTx on iNOS expression in BMDM (Fig. 9F). iNOS is dependent on K⁺ channel activity in macrophage-like cell lines (37), and similarly to IL-2 in T-cell (38), could be considered as a marker of macrophage activation (25, 35). LPS and TNF-α-induced activation triggered an increase in iNOS expression and the presence of 10 nM MgTx inhibited iNOS induction (Fig. 9F).

DISCUSSION

Since the early 1980s several laboratories have been characterizing ion channels in red blood cells and leukocytes. Several

46316   *Differential K⁺ Channel Regulation in Macrophages*

FIG. 7. **TNF-α up-regulates Kv1.3 and down-regulates Kir2.1 VDPC.** *A*, RT-PCR analysis of Kv1.3 and Kir2.1 mRNA expression at different times after TNF-α treatment. Results from RT-PCR on 0.25 μg of total RNA during 30 cycles for Kv1.3 and Kir2.1 and 0.1 μg of RNA and 10 cycles for 18 S are shown. These conditions were at the exponential phase of the amplicon production as described under "Experimental Procedures." ●, Kv1.3; ○, Kir2.1; ■, 18 S. Significant differences were found with Kv1.3 and Kir2.1 ($p < 0.001$, ANOVA). *B*, Kv1.3 and Kir2.1 Western blot analysis. Cells were incubated for 24 h with (*+TNF-α*) or without (*−TNF-α*) the cytokine. *Open bars*, Kv1.3; *closed bars*, Kir2.1; *hatched bars*, β-actin. *, $p < 0.05$; **, $p < 0.01$ *versus* −TNF-α (Student's *t* test). Representative filters are shown. Values are mean ± S.E. of four independent experiments.
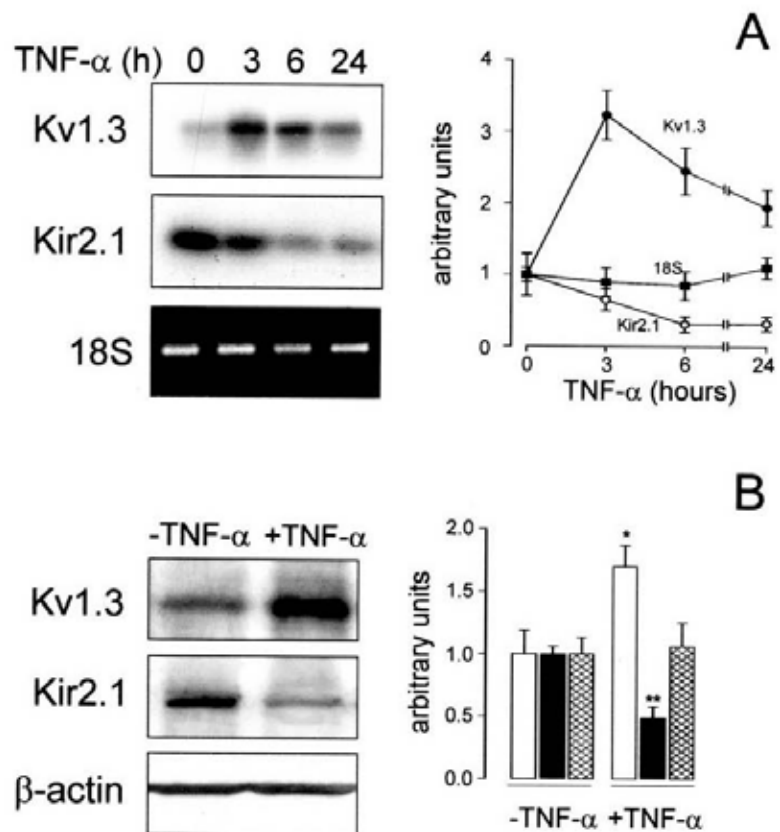
types of voltage-dependent sodium, chloride, proton, and potassium currents have been identified in macrophages of diverse origin. Among them, voltage-gated outward and inward K⁺ currents have been the most studied. In leukocytes, whereas outward K⁺ currents contribute to restoring membrane potential after depolarization, inward K⁺ currents have a key role after hyperpolarization (see Refs. 18–20 and 37 for reviews).

Voltage-dependent K⁺ Channels in Bone Marrow-derived Macrophages—The present study identifies for the first time the VDPC expressed in non-transformed macrophages. BMDM is a cell model that follows the physiological schedule within the body (2, 22, 25). Mature cells may proliferate or become activated after a specific stimulus. The use of dedifferentiated cell lines (THP-1 or HL-60 among others) as well as thioglycollate-elicited peritoneal macrophages, blood monocytes, or microglia has yielded controversial results (4–20, 39–42). Those data imply that K⁺ channels expressed in macrophages depend on the source and the differentiated status of the cells. Furthermore, the presence of K⁺ currents in BMDM had been reported but the proteins responsible had not been identified (42). Our results indicate that Kv1.3 is the main channel responsible for the outward current and Kir2.1 is responsible for the inward.

The presence of other candidates was tested in our model. Lymphocytes express several voltage-dependent K⁺ currents (*n*, *n′*, and *l*-type channels). While Kv1.3 is associated with the *n*-type channel and Kv3.1 accounts for the *l*-type, the protein responsible for the *n′*-type is unknown (38). In addition, other channels have been described in immune system cells. Thus, KCNE1 (also named Isk) was cloned from T-cells (43), Kv1.1 was found in CD4⁻CD8⁻ thymocytes (44) and Kv1.5 was iden-

tified in non-proliferating hippocampal microglia (45). We did not find Kv3.1 and Kv1.1 in macrophages by RT-PCR. Other related Kv1 channels such as Kv1.2 and Kv1.6 were also absent in our model. This result is consistent with the specific blockage of the outward current by MgTx and ShK-Dap²² even when cells proliferated or were activated. However, the expression of Kv1.5 indicates that heterotetrameric structures between Kv1.3 and Kv1.5 would be possible and should be considered.

M-CSF-dependent Proliferation Versus LPS-induced Activation—VDPC are implicated in proliferation and activation. Their role in G₁/S cell cycle progression has been reviewed, and their function in IL-2 secretion by T-lymphocytes has been demonstrated (38). However, different cell models produce controversial results. Whereas in some cell lines the differentiation is a prerequisite for VDPC expression, the macrophage phenotype often determines the loss of specific ion channel properties (18). Many studies have used B- and T-cells. However, lymphocyte activation leads to associated proliferation via autocrine production of IL-2 (38). In this cellular scenario, the physiological role of VDPC in the immune system remains to be determined.

We have found that M-CSF-dependent proliferation led to an increase in the K⁺ current conducted by Kv1.3. Links between proliferation and VDPC expression are supported by the cell growth arrest in the presence of K⁺ channel blockers (36, 46, this study). M-CSF activates phosphorylation cascades that involve Src homology 2 domains and induction of mitogen-activated protein kinase (24). Kv1.3 shows tyrosine kinase regulation and, in addition to its role as an ion channel, might be involved in the activation of Src-like tyrosine kinases that

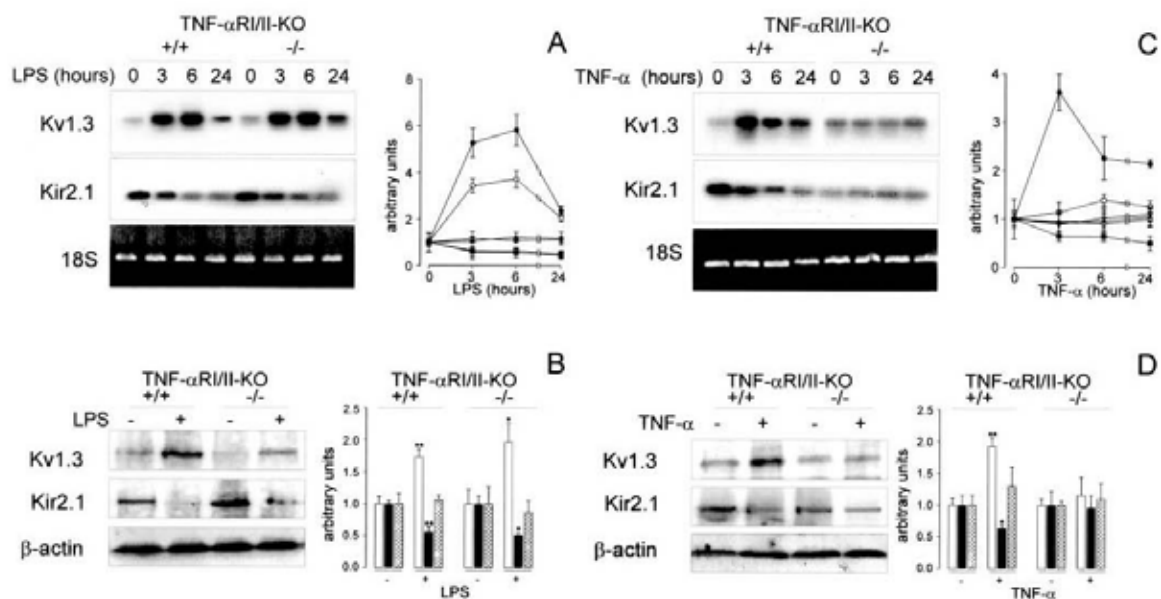Differential K⁺ Channel Regulation in Macrophages   46317

FIG. 8. **Evidence for TNF-α-independent mechanisms mediating the VDPC regulatory responses to LPS in macrophages.** Cells cultured in the absence of M-CSF for 19 h were incubated for a further 24 h in the presence of the growth factor supplemented with LPS or TNF-α. Samples from wild type (+/+) or TNF-α receptor I/II double knockout (−/−) mice were collected at the indicated times. A, RT-PCR analysis of Kv1.3 and Kir2.1 mRNA expression after LPS treatment. RT-PCR results were at the exponential phase of the amplicon production as described in the legend to Fig. 5. Significant differences were found in Kv1.3 and Kir2.1 ($p < 0.001$, ANOVA). ●, ○: Kv1.3; ■, □: Kir2.1; ▲, △: 18 S. *Closed symbols,* +/+; *open symbols,* −/−. B, Kv1.3 and Kir2.1 Western blot analysis. Cells were incubated for 24 h with (+LPS) or without (−LPS) the endotoxin. *Open bars,* Kv1.3; *closed bars,* Kir2.1; *hatched bars,* β-actin. *, $p < 0.05$; **, $p < 0.01$ *versus* −LPS (Student's t test). C, RT-PCR analysis of Kv1.3 and Kir2.1 mRNA expression after TNF-α treatment. RT-PCR results were at the exponential phase of the amplicon production as described in the legend to Fig. 7. *Symbols* are described in A. Kv1.3 and Kir2.1 significant differences were found only in +/+ macrophages ($p < 0.001$, ANOVA). D, Kv1.3 and Kir2.1 Western blot analysis. Cells were incubated for 24 h with (+TNF-α) or without (−TNF-α) the cytokine. Symbols are described in B. *, $p < 0.05$; **, $p < 0.01$ *versus* −TNF-α (Student's t test). Representative filters are shown. Values are mean ± S.E. of four independent experiments.

are important for cell growth (47, 48). However, our results go further, because we demonstrate that the long term increase in Kv1.3 activity is under *de novo* mRNA and protein synthesis, similarly to what was observed with the inward K⁺ current and Kir2.1. This is in contrast to what is described in phorbol 12-myristate 13-acetate-differentiated HL-60 cells or thioglycollate-elicited peritoneal macrophages (12). However, our results are in agreement with studies in which Ba²⁺ inhibits melanoma cell proliferation linked to a decrease in the membrane depolarization (28).

The question arises as to why macrophages need both K⁺ channels to proliferate. Whereas the Kv1.3 current could set the membrane potential at −50 to −60 mV, Kir2.1 would shift the potential to more negative values, close to the Nernst potassium equilibrium. A similar mechanism operates during myogenesis. Kir2.1 forces the potential to more negative values than hERG channels, leading to cell fusion mediated by Ca²⁺ (49). The degree of membrane hyperpolarization determines the extent of Ca²⁺ influx (49, 50). In macrophages, MgTx and Ba²⁺ inhibited proliferation and their combination was additive. In addition, MgTx and Ba²⁺ partially block proliferation in oligodendrocytes and melanoma cells (28, 36). These results have physiological significance because an increase in intracellular Ca²⁺ activates calcineurin, the translocator of the transcriptional factor NF-IL2A, the mitogen-activated protein II kinase, and the DNA synthesis promoting factor (38, 51). Consequently, by inducing Kv1.3 and Kir2.1, macrophages would maintain sufficiently negative potential to open Ca²⁺ channels and thus initiate mitotic Ca²⁺ signaling pathways.

LPS-induced activation blocks macrophage proliferation (25, 35) and regulates Kv1.3 and Kir2.1 under mRNA and protein

synthesis control. Previous studies show that K⁺ currents can be differentially regulated. Whereas granulocyte macrophage-CSF and LPS induce the outward current, without changes in Kv1.3 mRNA, the inwardly rectifying current decreased in microglia (19). In addition, transforming growth factor-β, a deactivating cytokine, induces Kv1.3 without any relevant effect on the inward current (52). In contrast, THP-1 phorbol 12-myristate 13-acetate-differentiated macrophages decreased Kv1.3 concomitantly to an increase in Kir2.1 (15). Our results suggest that LPS-induced activation regulates VDPC differentially, probably fine tuning the membrane potential and discriminating them from proliferative signals that require more negative values.

By inducing Kv1.3 and repressing Kir2.1, macrophages reduce the Ca²⁺ driving force, the intracellular K⁺ concentration ($[K^+]_i$), and the membrane potential hyperpolarization. While an increase in Ca²⁺ initiates the mitogenic pathway, LPS-induced activation does not mobilize Ca²⁺ in macrophages (53). LPS activates macrophages and generates apoptosis in several cell types (25). Kv1.3 functions relatively early in the pro-apoptotic cascade in T-cells and neurons (54, 55). In addition, a decrease in $[K^+]_i$ is involved in the formation of the apoptosome (56). This is consistent with the Kv1.3 and Kir2.1 regulation that we observed. Thus, a loss of cytosolic K⁺ is related to thymocyte apoptosis and partially protected by blocking K⁺ channels (57). On the other hand, VDPC blockers and depolarizing agents cause p27^{kip1} and p21^{cip1(waf-1)} accumulation and G₁ arrest in oligodendrocyte progenitors (58). Furthermore, a p21^{cip1(waf-1)} increase is associated with the cell growth inhibition in interferon-γ-activated macrophages (59). However, although p21^{cip1(waf-1)} could play a role in the inhibition of macro-

91

46318   *Differential K+ Channel Regulation in Macrophages*
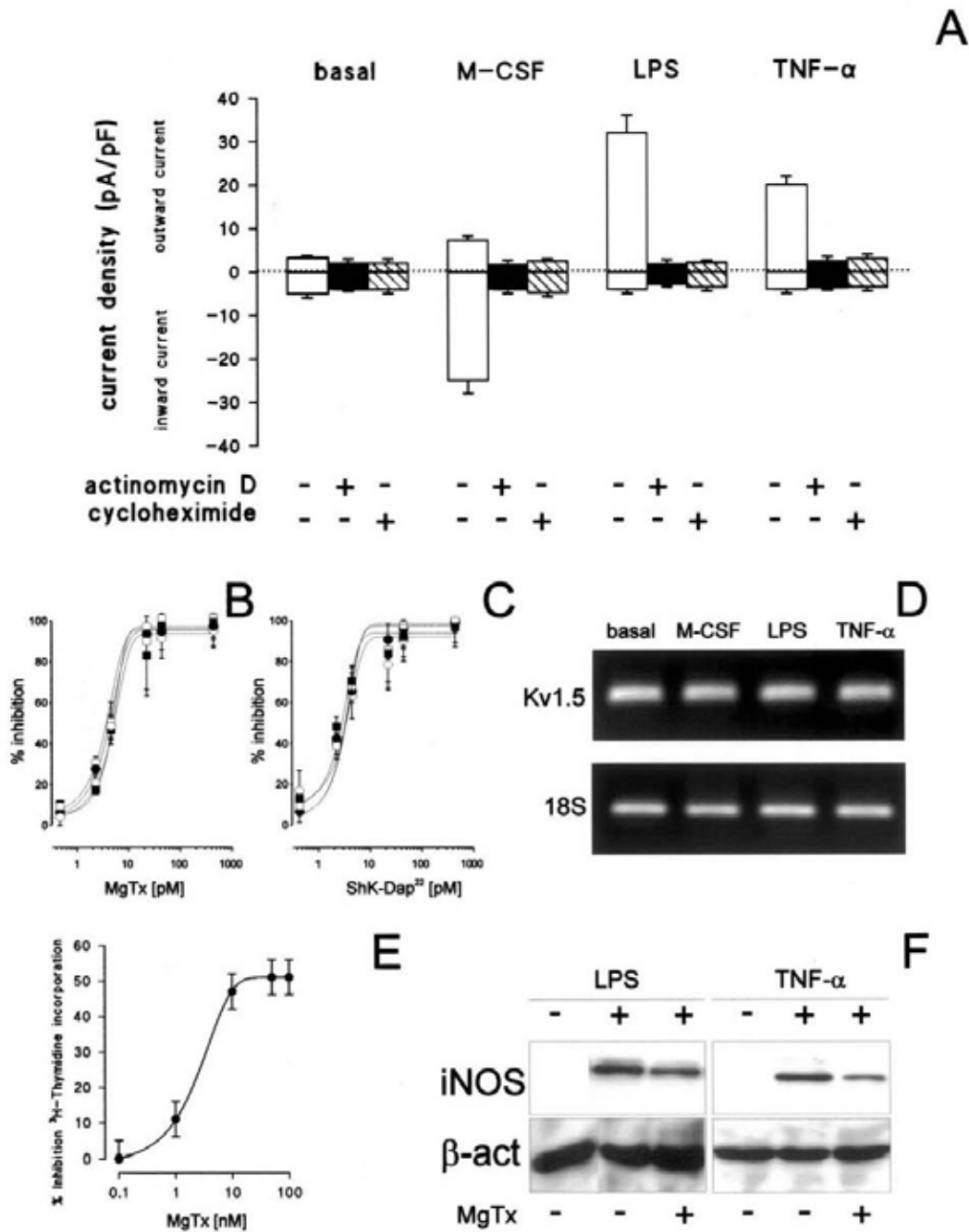

Fig. 9. **VDPC regulation is dependent on *de novo* mRNA and protein synthesis and Kv1.3 is involved in BMDM activation and proliferation.** Macrophages were cultured in the absence of M-CSF for 18 h, then G_0-arrested cells were further incubated for 24 h in the absence (*basal*) or presence of M-CSF with or without LPS or TNF-α. *A*, regulation of K+ currents is dependent on *de novo* synthesis of mRNA and protein. K+ current induction was inhibited by the addition of either 5 μg/ml actinomycin D (*closed bars*) or 5 μg/ml cycloheximide (*hatched bars*) during the treatment. Cells were held at -60 mV and currents were elicited by depolarizing pulses of $+50$ mV (outward current) and hyperpolarizing pulses of -150 mV (inward currents). Values are the mean $\pm$ S.E. of at least six independent cells. *B* and *C*, inhibition of the outward K+ current by MgTx and ShK-Dap^{22}, respectively. O, basal; ●, M-CSF; □, LPS; ■, TNF-α. *D*, Kv1.5 mRNA expression analyzed by RT-PCR in BMDM. See "Experimental Procedures" for details. *E*, MgTx inhibits M-CSF-dependent proliferation in macrophages. Macrophages were cultured in the absence of M-CSF for 18 h. Cells were further incubated during 24 h with or without the growth factor (1200 units/ml) in the presence of increasing concentrations of MgTx. Sample collection was performed as described under "Experimental Procedures." Values are the mean $\pm$ S.E. of four different assays each done in triplicate. *F*, Kv1.3 is involved in the LPS- and TNF-α-induced activation. Proliferating macrophages were cultured during 24 h in the absence ($-$) or presence ($+$) of LPS and TNF-α with or without 10 nM MgTx. iNOS protein expression was determined as described under "Experimental Procedures." A representative Western blot of three independent experiments is shown.

Differential K⁺ Channel Regulation in Macrophages   46319

phage proliferation by K⁺ channels, other mechanisms may be involved. Thus, cyclin D, essential for G_1/S progression, is regulated by extracellular signals (59). In this context, the induction of Kv1.3 associated with a Kir2.1 decrease would increase the extracellular K⁺ concentration. Similar depolarization activates T-cell β_1 integrin moieties initiating T-cell immune reactions (60).

Role of TNF-α—Most of the effects of LPS during endotoxic shock are associated with the secretion of TNF-α by tissue macrophages (25). TNF-α affects the growth and function of many cell types, and is a major mediator of inflammatory immune responses upon the activation of p55 type I and p75 type II receptors (61). Several lines of evidence implicate TNF-α in LPS-induced regulation of VDPC. First, TNF-α blocks proliferation and is involved in several LPS-induced mechanisms such as apoptosis and nucleoside transport (25, 35). Second, the time course of VDPC regulation probably coincides with the early induction of TNF-α mRNA expression (25). Finally, the production of TNF-α requires K⁺ channel activity (62).

TNF-α mimicked the LPS differential regulation of VDPC. However, this affirmation is only partially correct. Whereas the effects on Kir2.1 were similar, Kv1.3 showed some differences. Results on current densities and knockout mice suggest that LPS regulation involves TNF-α–dependent and -independent mechanisms. Indeed, TNF-α inhibits cell proliferation but the further addition of either MgTx or Ba²⁺ was additive.

In the bone marrow, TNF-α induces DNA fragmentation and cell death by apoptosis (25, 35). The activation of caspase 8 initiates the cascade of caspases that leads to apoptosis, apparently without any second messengers (25). However, alterations in ion composition regulate the activity of effector caspases and nucleases, thereby regulating pro-apoptotic signals (63). As indicated above, differential regulation of VDPC could modify this intracellular ion composition. Indeed, a +25 mV change modifies IL-2 production, thus reducing the activation and the antibody production by lymphocytes (50). Thus, differences between the LPS and TNF-α regulation of Kv1.3 and Kir2.1 currents could separate the two situations triggering the required and specific immune response.

Evidence for Post-translational Control of Kv1.3 during Activation—Ion channels are under extensive regulation, and changes among expression levels have been reported. However, in long term studies, VDPC mRNA mostly governs protein and activity (13, 34, 36). Although our results indicate that VDPC are mainly regulated at the transcriptional level, which is translated to protein abundance, which in turn would be responsible for changes in current amplitudes, other alternative mechanisms, such as changes in mRNA stability, should not be discarded.

While M-CSF-dependent proliferation did not modify the steady-state activation curves for Kv1.3 and Kir2.1, LPS and TNF-α reduced the *k* value of Kv1.3. Previous studies suggest that K⁺ channels are involved in T-cell activation and provide evidence of post-translational processes. Thus, Kv1.3 could be phosphorylated by several kinases (38, 47). In addition, conformational changes of the K⁺ channel structure are possible by high K⁺ concentrations outside the T-cell (60). Finally, the heteromeric structure of the Kv1.3 associated with Kv1.5 and Kvβ regulatory subunits could define a wide diversity of physiological activities and immunological functions (64). Indeed, LPS induces Kvβ1.1 and Kvβ2.1 in T-cells and splenocytes (65). Changes in Kvβ subunits during macrophage activation could indeed modify the kinetics of the *de novo* synthesized K⁺ channels as observed during myogenesis (34). Work is in progress in our laboratory to elucidate the role of these modulatory

subunits and some preliminary results have been recently described (66).

In summary, we provide strong evidence that proliferation and activation require specific VDPC modulation that would determine appropriate signals for each process. Furthermore, VDPC regulation by LPS implies redundant pathways in which the endotoxin participates by TNF-α-dependent and -independent mechanisms that would trigger differential responses. Our results have physiological significance because the channels might control the cell physiology and their activity may also be modulated by changes in the K⁺ gradient. Thus, a loss of $[K^+]_i$ occurs in immunologically relevant situations such as cellular injury, stress, and inflammation (60). In this context, VDPC could buffer K⁺ and modulate cellular responses. Finally, our results indicate that K⁺ channels should be considered as pharmacological targets in anti-inflammatory and immunomodulation therapies.

REFERENCES

1. Ogawa, M. (1993) *Blood* **81**, 2844–2853
2. Celada, A., and Nathan, C. (1993) *Immunol. Today* **15**, 100–102
3. Hille, B. (2001) *Ion Channels of Excitable Membranes*, 3rd Ed., Sinauer Associates, Sunderland, MA
4. Gallin, E. K., and Livengood, D. R. (1981) *Am. J. Physiol.* **241**, C9–C17
5. Gallin, E. K. (1984) *Biophys. J.* **46**, 821–825
6. Ypey, D. L., and Clapham, D. E. (1984) *Proc. Natl. Acad. U. S. A.* **81**, 3083–3087
7. Gallin, E. K., and Sheehy, P. A. (1985) *J. Physiol.* **369**, 475–499
8. Gallin, E. K., and McKinney, L. C. (1988) *J. Membr. Biol.* **103**, 55–66
9. McKinney, L. C., and Gallin, E. K. (1988) *J. Membr. Biol.* **103**, 41–53
10. Gallin, E. K. (1989) *Am. J. Physiol.* **257**, C77–C85
11. McKinney, L. C., and Gallin, E. K. (1992) *J. Membr. Biol.* **130**, 265–276
12. Judge, S. I., Montcalm-Mazzilli, E., and Gallin, E. K. (1994) *Am. J. Physiol.* **267**, C1691–C1698
13. DeCoursey, T. E., Kim, S. Y., Silver, M. R., and Quandt, F. N. (1996) *J. Membr. Biol.* **152**, 141–157
14. Eder, C., Klee, R., and Heinemann, U. (1997) *Naunyn-Schmiedeberg's Arch. Pharmacol.* **356**, 233–239
15. Schmid-Antomarchi, H., Schmid-Alliana, A., Romey, G., Ventura, M. A., Breittmayer, V., Millet, M. A., Husson, H., Moghrabi, B., Lazdunski, M., and Rossi, B. (1997) *J. Immunol.* **159**, 6209–6215
16. Colden-Stanfield, M., and Gallin, E. K. (1998) *Am. J. Physiol.* **275**, C267–C277
17. Qiu, M. R., Campbell, T. J., and Breit, S. N. (2002) *Clin. Exp. Immunol.* **130**, 67–74
18. Gallin, E. K. (1991) *Physiol. Rev.* **71**, 775–811
19. Eder, C. (1998) *Am. J. Physiol.* **275**, C327–C342
20. DeCoursey, T. E., and Grinstein, S. (1999) in *Inflammation: Basic Principles and Clinical Correlates* (Gallin, J. I., and Snyderman, R., eds) pp. 141–157, Lippincott Williams & Wilkins, Philadelphia, PA
21. Blunck, R., Scheel, O., Müller, M., Brandenburg, K., Seitzer, U., and Seydel, U. (2001) *J. Immunol.* **166**, 1009–1015
22. Soler, C., García-Manteiga, J., Valdés, R., Xaus, J., Comalada, M., Casado, F. J., Pastor-Anglada, M., Celada, A., and Felipe, A. (2001) *FASEB J.* **15**, 1979–1988
23. Stanley, E. R., Berg, K. L., Einstein, D. B., Lee, P. S., Pixley, F. J., Wang, Y., and Yeung, Y. G. (1997) *Mol. Reprod. Dev.* **46**, 4–10
24. Sweet, M. J., and Hume, D. A. (1996) *J. Leukocyte Biol.* **60**, 8–26
25. Xaus, J., Comalada, M., Valledor, A. F., Lloberas, J., López-Soriano, F. J., Argilés, J. M., Bogdan, C., and Celada, A. (2000) *Blood* **95**, 3823–3831
26. Garcia-Calvo, M., Leonard, R. J., Novick, J. N., Stevens, S. P., Schmalhofer, W., Kaczorowski, G. J., and Garcia, M. L. (1993) *J. Biol. Chem.* **268**, 18866–18874
27. Kalman, K., Pennington, M. W., Lanigan, M. D., Nguyen, A., Rauer, H., Mahnir, V., Paschetto, K., Kem, W. R., Grissmer, S., Gutman, G. A., Christian, E. P., Cahalan, M. D., Norton, R. S., and Chandy, K. G. (1998) *J. Biol. Chem.* **273**, 32697–32707
28. Lepple-Wienhues, A., Berweck, S., Böhmig, M., Leo, C. P., Meyling, B., Garbe, C., and Wiederholt, M. (1996) *J. Membr. Biol.* **151**, 149–157
29. Celada, A., Klemsz, M. J., and Maki, R. A. (1989) *Eur. J. Immunol.* **19**, 1103–1109
30. Cullel-Young, M., Barrachina, M., López-López, C., Goñalons, E., Lloberas, J., Soler, C., and Celada, A. (2001) *Immunogenetics* **53**, 136–144
31. Bruce, A. J., Boling, W., Kindy, M. S., Peschon, J., Kraemer, P. J., Carpenter, M. K., Holtsberg, F. W., and Mattson, M. P. (1996) *Nat. Med.* **2**, 788–794
32. Fuster, G., Vicente, R., Coma, M., Grande, M., and Felipe, A. (2002) *Methods Find. Exp. Clin. Pharmacol.* **24**, 253–259

46320   *Differential K⁺ Channel Regulation in Macrophages*

33. Coma, M., Vicente, R., Busquets, S., Carbó, N., Tamkun, M. M., López-Soriano, F. J., Argilés, J. M., and Felipe, A. (2003) *FEBS Lett.* **536**, 45–50
34. Grande, M., Suárez, E., Vicente, R., Cantó, C., Coma, M., Tamkun, M. M., Zorzano, A., Gumà, A., and Felipe, A. (2003) *J. Cell. Physiol.* **195**, 187–193
35. Soler, C., Valdés, R., García-Manteiga, J., Xaus, J., Comalada, M., Casado, F. J., Modolell, M., Nicholson, B., MacLeod, C., Felipe, A., Celada, A., and Pastor-Anglada, M. (2001) *J. Biol. Chem.* **276**, 30043–30049
36. Chittajallu, R., Chen, Y., Wang, H., Yuan, X., Ghiani, C. A., Heckman, T., McBain C. J., and Gallo, V. (2002) *Proc. Natl. Acad. Sci. U. S. A.* **99**, 2350–2355
37. Lowry, M. A., Goldberg, J. I., and Belosevic, M. (1998) *Clin. Exp. Immunol.* **111**, 597–603
38. Cahalan, M. D., Wulff, H., and Chandy, K. G. (2001) *J. Clin. Immunol.* **21**, 235–252
39. Wieland, S., Chou, R. H., and Gong, Q. H. (1990) *J. Cell. Physiol.* **142**, 643–651
40. Nelson, D. J., Jow, B., and Jow, F. (1992) *J. Membr. Biol.* **125**, 201–218
41. Lu, L., Yang, T., Markakis, D., Guggino, W. B., and Craig, R. W. (1993) *J. Membr. Biol.* **132**, 267–274
42. Eder, C., and Fischer, H. G. (1997) *Arch. Pharmacol.* **355**, 198–202
43. Attali, B., Romey, G., Honoré, E., Semid-Alliana, A., Mattéi, M. G., Lesage, F., Ricard, P., Barhanin, J., and Lazdunski, M. (1992) *J. Biol. Chem.* **267**, 8650–8657
44. Freedman, B. D., Fleischmann, B. K., Punt, J. A., Gaulton, G., Hashimoto, Y., and Kotlikoff, M. I. (1995) *J. Biol. Chem.* **270**, 22406–22411
45. Kotecha, S. A., and Schlichter, L. C. (1999) *J. Neurosci.* **19**, 10680–10693
46. Sobko, A., Perezt, A., Shirihai, O., Etkin, S., Cherepanova, V., Dagan, D., and Attali, B. (1998) *J. Neurosci.* **18**, 10398–10408
47. Holmes, T. C., Fadool, D. A., and Levitan, I. B. (1996) *J. Neurosci.* **16**, 1581–1590
48. Holmes, T. C., Berman, K., Swartz, J. E., Dagan, D., and Levitan, I. B. (1997) *J. Neurosci.* **17**, 8964–8974
49. Fischer-Lougheed, J., Liu, J. H., Espinos, E., Mordasini, D., Bader, C. R., Belin, D., and Bernheim, L. (2001) *J. Cell Biol.* **153**, 677–685
50. Freedman, B. D., Price, M. A., and Deutsch, C. J. (1992) *J. Immunol.* **149**, 3784–3794
51. Berridge, M. J. (1993) *Nature* **361**, 315–325
52. Schilling, T., Quandt, F. N., Cherny, V. V., Zhou, W., Heinemann, U., DeCoursey, T. E., and Eder, C. (2000) *Am. J. Physiol.* **279**, C1123–C1134
53. Valledor, A. F., Xaus, J., Comalada, M., Soler, C., and Celada, A. (2000) *J. Immunol.* **164**, 29–37
54. Bock, J., Szabó, I., Jekle, A., and Gulbins, E. (2002) *Biochem. Biophys. Res. Commun.* **295**, 526–531
55. Yu, S. P., Yeh, C. H., Gottron, F., Wang, X., Grabb, M. C., and Choi, D. W. (1999) *J. Neurochem.* **73**, 933–941
56. Cain, K., Langlais, C., Sun, X. M., Brown, D. G., and Cohen, G. M. (2001) *J. Biol. Chem.* **276**, 41985–41990
57. Dallaporta, B., Marchetti, P., de Pablo, M. A., Maisse, C., Duc, H. T., Métivier, D., Zamzami, N., Geuskens, M., and Kroemer, G. (1999) *J. Immunol.* **162**, 6534–6542
58. Ghiani, C. A., Yuan, X., Eisen, A. M., Knutson, P. L., DePinho, R. A., McBain, C. J., and Gallo, V. (1999) *J. Neurosci.* **19**, 5380–5392
59. Xaus, J., Cardó, M., Valledor, A. F., Soler, C., Lloberas, J., and Celada, A. (1999) *Immunity* **11**, 103–113
60. Levite, M., Cahalon, L., Peretz, A., Hershkoviz, R., Sobko, A., Ariel, A., Desai, R., Attali, B., and Lider, O. (2000) *J. Exp. Med.* **191**, 1167–1176
61. Tartaglia, L. A., and Goeddel, D. V. (1992) *Immunol. Today* **13**, 151–153
62. Maruyama, N., Kakuta, Y., Yamauchi, K., Ohkawara, Y., Aizawa, T., Ohrui, T., Nara, M., Oshiro, I., and Tamura, G. (1994) *Am. J. Respir. Cell Mol. Biol.* **10**, 514–520
63. Bortner, C. D., and Cidlowski, J. A. (1999) *J. Biol. Chem.* **274**, 21953–21962
64. McCormack, T., McCormack, K., Nadal, M. S., Vieira, E., Ozaita, A., and Rudy, B. (1999) *J. Biol. Chem.* **274**, 20123–20126
65. Autieri, M. V., Belkowski, S. M., Constantinescu, C. S., Cohen, J. A., and Prystowsky, M. B. (1997) *J. Neuroimmunol.* **77**, 8–16
66. Vicente, R., Escalada, A., Coma, M., Grande, M., Fuster, G., López-Iglesias, C., Solsona, C., and Felipe, A. (2003) *J. Physiol.* **548P**, O20

13204   *Additions and Corrections*

Vol. 278 (2003) 46307–46320

Differential voltage-dependent K⁺ channel responses during proliferation and activation in macrophages.

Rubén Vicente, Artur Escalada, Mireia Coma, Gemma Fuster, Ester Sánchez-Tilló, Carmen López-Iglesias, Concepió Soler, Carles Solsona, Antonio Celada, and Antonio Felipe

Page 46312, under "Results": Lines 36 and 37 from the top. Because margatoxin and ShK-Dap22 were 10 times more concentrated than originally described, the IC_{50} values for inhibition were ~50 and ~30 pM for MgTx and ShK-Dap22, respectively.

Vol. 279 (2004) 13764–13768

Glycogen synthase sensitivity to glucose-6-P is important for controlling glycogen accumulation in *Saccharomyces cerevisiae*.

Bartholomew A. Pederson, Wayne A. Wilson, and Peter J. Roach

Page 13764, Abstract and Introduction: R579A/R581A/R582A, used to designate a mutant form of glycogen synthase, should be replaced with R579A/R580A/R582A throughout.

The systemic inflammatory response is involved in the regulation of K⁺ channel expression in brain via TNF-α-dependent and -independent pathways

Rubén Vicente[a,1], Mireia Coma[a,1], Silvia Busquets[b], Rodrigo Moore-Carrasco[b], Francisco J. López-Soriano[b], Josep M. Argilés[b], Antonio Felipe[a,*]

[a]*Molecular Physiology Laboratory, Departament de Bioquímica i Biologia Molecular, Universitat de Barcelona, Avda. Diagonal 645, E-08028 Barcelona, Spain*
[b]*Cancer Research Group, Departament de Bioquímica i Biologia Molecular, Universitat de Barcelona, Avda. Diagonal 645, E-08028 Barcelona, Spain*

Abstract TNF-α, generated during the systemic inflammatory response, triggers a wide range of biological activities that mediate the neurologic manifestations associated with cancer and infection. Since this cytokine regulates ion channels in vitro (especially Kv1.3 and Kir2.1), we aimed to study Kv1.3 and Kir2.1 expression in brain in response to in vivo systemic inflammation. Cancer-induced cachexia and LPS administration increased plasma TNF-α. Kv1.3 and Kir2.1 expression was impaired in brain during cancer cachexia. However, LPS treatment induced Kv1.3 and downregulated Kir2.1 expression, and TNF-α administration mimicked these results. Experiments using TNF-α double receptor knockout mice demonstrated that the systemic inflammatory response mediates K⁺ channel regulation in brain via TNF-α-dependent and -independent redundant pathways. In summary, distinct neurological alterations associated with systemic inflammation may result from the interaction of various cytokine pathways tuning ion channel expression in response to neurophysiological and neuroimmunological processes.
© 2004 Federation of European Biochemical Societies. Published by Elsevier B.V. All rights reserved.

Keywords: K⁺ channels; Cancer cachexia; Systemic inflammatory response; Brain; TNF-α; Lipopolysaccharide

1. Introduction

Systemic inflammation represents a pleiotropic mechanism generated in response to a number of body insults. Trauma, AIDS, drug abuse, infection and cancer are often associated with this pathological condition through the production of inflammatory cytokines, TNF-α being one of the most relevant. The administration of lipopolysaccharide (LPS) or pro-inflammatory cytokines to animals mimics several catabolic aspects of cancer-induced cachexia [1,2]. Cytokines act in paracrine, autocrine and intracrine manners, and are often difficult to detect in the circulation. In fact, paracrine interactions are a predominant cytokine mode of action within organs, including the brain. In the central nervous system, the direct action of cytokines in neuronal cells either increases or decreases neuronal activity, while in other nerve cell types, it can activate an immunological/inflammatory response. In certain pathophysiological conditions, cytokine cascades lead to neurotoxicity and neurodegeneration [3].

LPS, a gram-negative bacterial endotoxin, has been extensively used for experimental induction of an inflammatory response; it causes anorexia and fever, and increases TNF-α production in rodents [4,5]. On the other hand, experimentally induced cancer-cachexia is a pathological state also characterized by a significant increase in TNF-α blood levels [6]. This cytokine possesses a wide range of biological activities. In the nervous system, TNF-α exerts cytotoxic effects on oligodendrocytes and affects myelin functions [7]. In addition, the concentration of TNF-α in brain tissues or serum is enhanced in neurodegenerative disorders such as Parkinson's and Alzheimer's diseases [8,9]. Thus, the central nervous system (CNS) is a clear target for cytokines involved in the inflammatory response. In this context, in vivo characterization of the molecular mechanisms responsible for the neurological manifestations triggered by the systemic inflammatory response is a key issue. One such mechanism involves the modulation of ion channels.

Neuronal K⁺ channels (KCh) form a large and diverse group that governs many physiological functions, e.g., resting membrane potential, action potential duration and frequency, and neurotransmitter release [10]. Voltage-dependent currents are mainly mediated by *Shaker*-like potassium channels (Kv), whereas inward currents are conducted by inward rectifier K⁺ channels (Kir). In CNS excitability, Kv repolarizes the membrane potential following a depolarizing stimulus. However, Kir stabilizes the resting membrane potential near the K⁺ equilibrium potential and mediates K⁺ transport across membranes [10].

The few in vitro studies that have analyzed the physiological effects of TNF-α on KCh show controversial results [11–14]. In this regard, we have described how Kv1.3 and Kir2.1 are regulated by LPS via TNF-α-dependent and -independent mechanisms in macrophages [15]. We have also reported that

*Corresponding author. Fax: +34-934021559.
E-mail address:* afelipe@ub.edu (A. Felipe).

[1] These authors contributed equally to this study.

the activity of both channels is needed for the fine tuning of the immunological response. Kv1.3 is involved in macrophage-induced activation by LPS and TNF-α [15]. It is also present in brain and given its biophysical activity, it has been related to the control of the neuronal firing pattern [16]. Moreover, Kir2.1 is also widely expressed in nerve cells with a relevant role in neuronal excitability and glial K$^+$ transport [17]. Although experimental cancer-induced cachexia downregulates the expression of Kv channels (i.e., Kv1.3) in brain, there is no information on Kir2.1 regulation or whether impaired Kv expression is directly related to the generation of a systemic inflammatory response [6].

Bearing all this in mind, we aimed to study the expression of the strongly inwardly rectifying potassium channel Kir2.1 in experimental cancer-induced cachexia and to evaluate whether KCh regulation is related to the rise in blood TNF-α levels during the systemic inflammatory response in vivo. In this context, since no in vivo studies have been reported, we followed several related approaches: (i) experimental cancer-induced cachexia by a rapidly growing tumor; (ii) TNF-α chronic administration and (iii) LPS administration using wild-type and TNF-α double receptor knockout (TNF-α RI/II-KO) mice. We show that the systemic inflammatory response regulates Kv1.3 and Kir2.1 channels differentially and that this modulation is mediated via TNF-α-dependent and -independent redundant pathways. Our results suggest that the differential expression of KCh subunits in the brain is crucial to achieving the correct neural activity in the systemic inflammatory response.

2. Materials and methods

2.1. Animals and experimental design

Several experimental groups of at least five animals each were used. Animals from Iffa-Credo (France) were fed ad libitum on a regular chow diet with free access to drinking water.

Experimental cancer-induced cachexia: Female Wistar rats (∼200 g) were injected intraperitoneally with a Yoshida AH-130 ascites hepatoma cell suspension (approx. 10^8 cells in 2 ml). Control rats were injected with 0.9% (w/v) NaCl solution (physiological saline) as described [6]. All extractions were performed 7 days after tumor transplantation.

TNF-α treatment: Female Wistar rats (∼200 g) were injected twice a day with recombinant-derived human TNF-α (50 μg/kg, i.p.) for 4 days [18]. Control animals followed the same schedule receiving saline.

LPS treatment: C57BL/6 mice of about 20 weeks of age were used. TNF-α RI/II-KO mice kindly provided by Hoffmann LaRoche were generated and characterized as reported [19,20]. Purified LPS (*Escherichia coli* endotoxin 0111:B4) was dissolved in pyrogen-free saline. Animals were injected intraperitoneally at a dose of 2.5 mg/kg. Animals kept at thermoneutral temperature (30 °C) developed fever 23 h after the LPS injection (data not shown, [21]). Another set of wild type and TNF-α RI/II-KO mice was used to administrate TNF-α (100 μg/kg, i.v.) as previously described [22 24]. In all cases, control mice received sterile saline.

2.2. Samples and TNF-α measurements

Blood was collected from killed animals and the plasma was obtained by centrifugation and quickly frozen. In all cases, tissue samples were removed and weighed at the end of the treatment. The brain and the heart were immediately frozen with liquid nitrogen and maintained at −80 °C until use. Animal handling procedures were approved by the Ethics committee of the University of Barcelona.

Plasma TNF-α was measured by using an ELISA test (Genzyme Corp.) following the manufacturer's instructions.

2.3. RNA extraction, cDNA probes, constructs, reverse transcription-polymerase chain reaction (RT-PCR) and Southern blot

Total RNA from brain and heart was isolated using Tripure (Roche Diagnostics). Samples were further treated with the DNA-free kit from Ambion Inc. to remove DNA. RNA from at least five animals was analyzed per group.

Ready-to-Go RT-PCR Beads (Amersham Pharmacia Biotech) were used in a one-step RT-PCR. Total RNA and Kv1.3, Kir2.1 and 18S primers were added to the beads as described [15]. A range of PCR cycles and RNA dilutions from each independent sample were performed to obtain an exponential phase of amplicon production (data not shown) as described [25]. The same independent RNA aliquot was used to analyze the KCh mRNA expression and the respective amount of 18S rRNA.

Once the exponential phase of the amplicon production had been determined, the specificity of each product was confirmed in test RT-PCRs using the appropriate cDNA probe in a Southern blot analysis [26]. PCR-generated KCh cDNA probes from mouse brain were used as probes as described [15]. At least three filters were prepared from independent samples and representative blots are shown. The densitometric analysis of the blots was performed using Phoretix software (Nonlinear Dynamics). Results are the means ± S.E.M. of each experimental group. Where indicated, statistical analysis by Student's *t* test was performed.

2.4. Membrane preparation and Western blot analysis

Brain samples were homogenized in 320 mM sucrose, supplemented with 1 μg/ml aprotinin, 1 μg/ml leupeptin, 86 μg/ml iodoacetamide and 1 mM phenylmethylsulfonyl fluoride as protease inhibitors in a glass homogenizer. An enriched membrane preparation was obtained [27]. Briefly, homogenates were centrifuged at 2000 × g for 5 min and the supernatant was further centrifuged at ∼100000 × g for 1 h. The pellet was resuspended in the same solution and protein content was determined by Bio-Rad Protein Assay (Bio-Rad). Samples were aliquoted and stored at −80 °C.

Crude membrane protein samples (50 μg) were boiled in Laemmli SDS loading buffer and separated on 10% SDS PAGE. They were transferred to nitrocellulose membranes (Immobilon-P, Millipore) and blocked in 5% dried milk-supplemented 0.2% Tween 20 PBS before immunoreaction. To monitor Kv1.3 and Kir2.1 expression, rabbit polyclonal antibodies (Alomone Labs) were used. As a loading and transfer control, a monoclonal anti-β-actin antibody (Sigma) was used.

3. Results and discussion

The generation and release of proinflammatory cytokines are among the main features of the systemic inflammatory response. In particular, TNF-α is a pleiotropic cytokine that plays a pivotal role in inflammatory diseases of the central nervous system [3,11,12]. It is generated mostly by macrophages in response to an insult and is a major mediator of the septic shock syndrome induced by either LPS or bacterial superantigens [20]. In addition, high levels of TNF-α have also been detected in neurodegenerative disorders [8,9]. Bearing this in mind, the aim of the present work was to analyze the potential role of TNF-α regulating KCh expression in brain during a systemic inflammatory response.

The results presented in Fig. 1 show plasma TNF-α concentration in two models of systemic inflammatory response, a model of experimental induced cancer-cachexia and in another model involving LPS administration. Rats that efficiently developed the Yoshida AH-130 tumor showed an increase in plasma cytokine concentration. On the other hand, LPS treated mice also showed high TNF-α levels in plasma, as reported elsewhere [28,29]. During cancer cachexia, the systemic TNF-α concentration increases concomitantly with tumor progression, while LPS rapidly increases plasma TNF-α within the first 2–3 h with a progressive decay over the next 24 h (data not
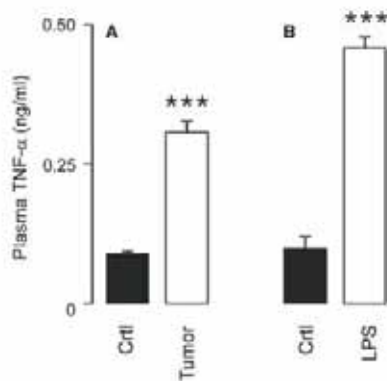
Fig. 1. Experimental cancer cachexia and LPS administration increased plasma TNF-α levels. (A) Wistar rats were injected intraperitoneally with saline (Crtl) or Yoshida AH-130 ascites hepatoma cell suspension (Tumor) as described in Section 2. Samples were collected 7 days after tumor transplantation. (B) Some C57BL/6 mice were injected intraperitoneally (2.5 mg/kg) with purified LPS in saline (LPS). Control mice (Crtl) received an equivalent volume of sterile saline as described in Section 2. Blood samples were collected 3 h after LPS administration. Values are means±S.E.M. of five animals. *** $P < 0.001$ vs. Crtl (Student's t test).

shown, [2]). These results indicate that both situations share a significant rise in circulating TNF-α triggering the catabolic inflammatory response.

Several neurodegenerative disorders, such as Parkinson's and Alzheimer's diseases share a systemic inflammatory response, similar to that we observed [8,9]. In these pathological conditions, nerve KCh are implicated in the neural response. Thus, β-amyloid peptide regulates the expression of KCh in microglia by upregulating Kv1.3 and Kv1.5 with no effects on Kir channels [30]. Kv channels (i.e., Kv1.3) repolarize the membrane potential after depolarization. However, Kir channels stabilize the resting membrane potential near the K⁺ equilibrium potential and mediate K⁺ transport across membranes. This role is crucial in the case of the strongly inward rectifier Kir2.1, which participates in the intrusion of K⁺ ions released from nerve axons. An increase in extracellular K⁺ may induce uncontrolled hyperexcitability and abnormal synchronization of neurons [17]. Experimental cancer cachexia specifically downregulated Kir2.1 as observed with Kv1.3 [6, Fig. 2]. Kv1.3 mRNA expression is impaired in the brain of tumor-bearing animals [6]. Here, we confirm and extend these results by reporting a parallel decrease in Kv1.3 protein in crude membrane samples from brain (Fig. 2B). The Kir2.1 downregulation observed in brain seems to be tissue-specific. This result may seem puzzling, since cancer cachexia is char-
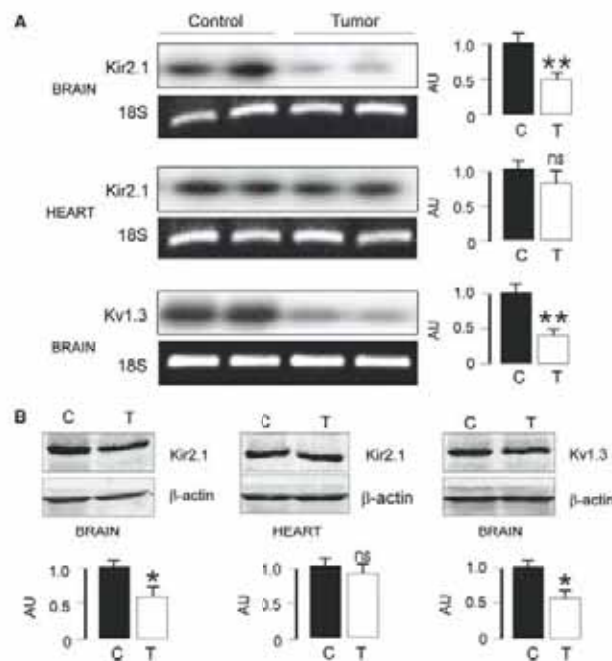

Fig. 2. Expression of Kv1.3 and Kir2.1 in brain and heart from animals under experimental cancer cachexia. At least five animals were inoculated with either saline (Control) or the Yoshida AH-130 ascites hepatoma cell suspension (Tumor) as described in Section 2. Total RNA and membrane protein samples were analyzed for K⁺ channel expression after 7 days of tumor growth. (A) Kir2.1 and Kv1.3 mRNA expression. Results from RT-PCR on 0.25 μg and 1 μg for brain and heart, respectively, and 30 cycles for Kir2.1 and Kv1.3, and 0.1 μg and 10 cycles for 18S are shown. These conditions were at the exponential phase of the amplicon production as described in Section 2. (B) Kir2.1 and Kv1.3 Western blot analysis. Representative blots are shown. Arbitrary unit (AU) values the means±S.E.M. of at least four animals. Closed bars, Control (C); open bars, tumor-bearing animals (T). *$P < 0.05$; **$P < 0.01$; ns, not significant vs. control (Student's t test).
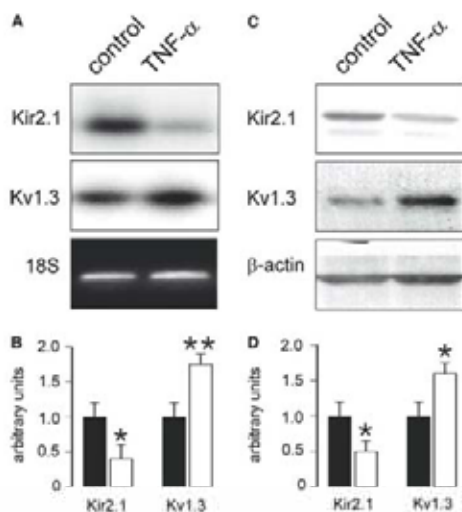
192

Fig. 3. Expression of Kv1.3 and Kir2.1 in brain from TNF-α-treated animals. At least five animals were administered intraperitoneally with either saline (control) or recombinant-derived human TNF-α (TNF-α) for 4 days. Animals were administered in two daily injections of 50 µg/kg (total dose of 100 µg/kg per day) for 4 days as described in Section 2. (A) Kir2.1 and Kv1.3 mRNA expression. Results from RT-PCR on 0.25 µg and 30 cycles for Kir2.1 and Kv1.3, and 0.1 µg and 10 cycles for 18S are shown. These conditions were at the exponential phase of amplicon production as described in Section 2. (B) Kir2.1 and K+1.3 mRNA expression values derived from panel A. (C) Kir2.1 and K+1.3 Western blot analysis. Representative blots are shown. (D) Kir2.1 and Kv1.3 protein expression values derived from panel C. In all cases, arbitrary units are standardized to the control value in the absence of TNF-α. Values are means ± S.E.M. of at least four animals. Closed bars, control; open bars, TNF-α-treated animals. *$P < 0.05$; **$P < 0.01$ vs. control (Student's t test).

acterized by muscle wasting [2]. However, the physiological role for Kir2.1 in muscle and brain may differ. In this context, the CNS responds to acute inflammation differently from other body tissues. In fact, calcium channels are regulated differentially in cardiac and neuronal cells [31]. Moreover, evidence indicates that unlike other well-known neurological disorders [3], the heart dysfunction that initiates with the syndrome may be peripheral [1].

Since plasma TNF-α levels increased during experimental cancer cachexia and may be responsible for impaired KCh expression in brain, we performed a set of experiments injecting TNF-α to rats. Previous studies from our group have clearly indicated that this chronic TNF-α administration mimics most of the metabolic alterations formed during experimental cancer cachexia. However, after 4 days of treatment, animals develop tolerance to the cytokine (see [2] for review). TNF-α differentially regulated Kv1.3 and Kir2.1 channels in brain (Fig. 3). In contrast to cancer cachexia, while Kir2.1 expression decreased, Kv1.3 was upregulated. These results may be interpreted taking into consideration certain key differences between the two models. Thus, while experimental cancer cachexia is a non-reversible situation in which brain cells undergo apoptosis [6], the increase in plasma TNF-α by chronic administration of the cytokine may be reversible, as it is during infection. Moreover, K+ channel expression is impaired in the brain during experimental cancer cachexia, and

animals lose weight and develop anorexia [6]. In addition, some K+ channel gene knockout mice lost body weight and showed altered feeding behavior [32,33]. However, chronic TNF-α administration does not affect food intake or body mass [18]. Other factors may explain the discrepancy between these two models. Thus, during experimental induced cancer-cachexia, the long term increase in plasma TNF-α could desensitize TNF-α receptors or upregulate the soluble forms of the receptor (sTNFR). In fact, high plasma levels of sTNFR have been found in patients with advanced gastrointestinal cancer and sTNFR is an agonist of TNF-α that could prevent some cytokine effects [34–37].

TNF-α is produced by lymphocytes and macrophages in response to an insult [20]. Within the brain, not only microglia but also activated leukocytes generate TNF-α locally [3]. As a result, there is an inflammatory response similar to that described in AIDS patients in which TNF-α expression correlates with the degree of dementia [38]. Few in vitro studies have reported differential K+ channel regulation by TNF-α in nerve cells, with controversial results, e.g., enhanced, unaltered and reduced outward and inward K+ currents [11–14]. However, the proteins responsible have not been identified. In addition, a differential Kv1.3 and Kir2.1 regulation by TNF-α in the brain is not surprising. In fact, our results agree with those described in bone marrow and brain macrophages [15,39].

During an infection, LPS is one of the strongest activators of macrophages and leads to the secretion of TNF-α. The generation of this and other cytokines such as IL-1β, IL-6 and IL-12 leads to a rapid systemic inflammatory response in the host. As mentioned above, LPS administration increases the systemic TNF-α concentration (Fig. 1). Despite the amount of information on how LPS affects KCh in in vitro studies [15,40,41], there are few in vivo studies. Exposure to sub-lethal doses of LPS evokes a systemic inflammatory response that includes fever and increased oxygen consumption similar to that described in certain types of cancer [21]. In acute inflammatory response, KCh were differentially regulated (Fig. 4). Kv1.3 expression was induced, whereas Kir2.1 was downregulated as observed with TNF-α. Several LPS effects are mediated by the production of TNF-α. Bearing this in mind, we aimed to test whether this modulation depended on the cytokine. For this purpose, we used TNF-α RI/II-KO mice, which received an acute LPS injection as mentioned above. While Kv1.3 upregulation was TNF-α-dependent, Kir2.1 modulation was independent (Fig. 4). These results are in agreement with those described using macrophages, which indicate that the LPS modulation of Kir2.1 is independent of TNF-α, whereas Kv1.3 regulation could be partially dependent [15]. However, TNF-α may also promote physiological effects by pathways independent of TNF-α receptors via its lectin binding domain [42,43]. This possibility was tested by injecting TNF-α into wild-type and TNF-α RI/II-KO mice. This treatment, which generates important metabolic alterations [22–24], did not modify KCh expression in the brain of TNF-α RI/II-KO mice. However, the effects in wild-type animals were similar to those found with LPS (data not shown). Taken together, these data suggest that LPS involves TNF-α-dependent and -independent redundant mechanisms in a number of cases. In fact, not only KCh but also nucleoside transport regulation may require this mode of action [44]. In addition, LPS-induced apoptosis involves TNF-α as an early step followed by induction of nitric oxide synthase [20]. In this regard, cancer may

100

R. Vicente et al. / FEBS Letters 572 (2004) 189 194   193
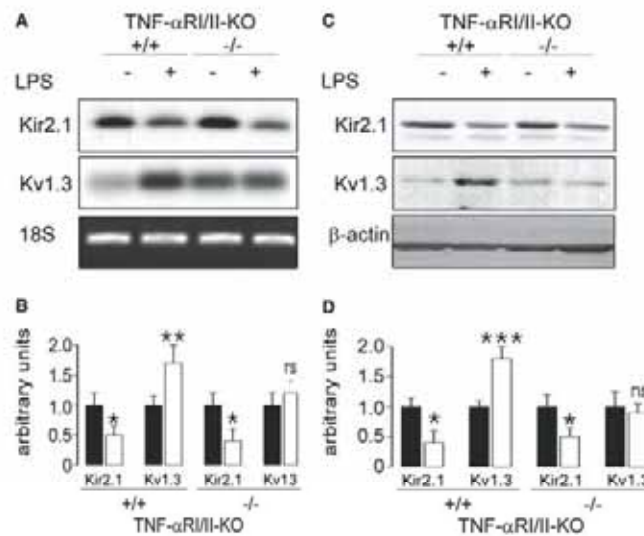

Fig. 4. Expression of Kv1.3 and Kir2.1 in brain from LPS-treated animals. At least five C57BL/6 wild type (+/+) or TNF-α receptor I/II double knockout (−/−) mice were administered intraperitoneally with either saline (−) or 2.5 mg/kg LPS (+). Animals were kept at thermoneutral temperature (30 °C) and samples were collected 23 h after LPS injection (A) Kir2.1 and Kv1.3 mRNA expression. Results from RT-PCR on 0.25 μg and 30 cycles for Kir2.1 and Kv1.3, and 0.1 μg and 10 cycles for 18S are shown. These conditions were at the exponential phase of the amplicon production as described in Section 2. Representative blots are shown. (B) Kir2.1 and Kv1.3 mRNA expression values derived from panel A (C) Kir2.1 and Kv1.3 Western blot analysis. Representative blots are shown. (D) Kir2.1 and Kv1.3 protein expression values derived from panel C. In all cases, arbitrary units are standardized to the control value in the absence of LPS (−). Values are means ± S.E.M. of at least four animals. Closed bars, control; open bars, LPS-treated animals. No significant differences were found between wild type (+/+) and TNF-α receptor I/II double knockout (−/−) mice in the absence of TNF-α (−). *P < 0.05; **P < 0.01; ***P < 0.001; ns, not significant vs. control (Student's t test).

induce oxidative stress within the brain, which has been related to the appearance of neurological disorders [45]. Once cytokine production is activated within the brain, paracrine and autocrine interactions can sustain local cytokine production through positive-feedback systems [3].

In summary, the systemic inflammatory response may be responsible for KCh regulation in brain. Blood TNF-α levels during the endotoxic shock may trigger a finely tuned modulation of KCh in the neurological response. Moreover, redundant TNF-α-dependent and -independent mechanisms are probably involved. The apparent discrepancy between infection and experimental cancer cachexia is not an irrelevant issue. On the contrary, it is indicative of quite different catabolic conditions. Upon experimental cancer cachexia, brain cells undergo apoptosis [6], which leads to neurotoxicity and neurodegeneration [3]. In contrast, acute inflammation caused by LPS may induce various responses within the brain that may lead to distinct neurological disfunctions.

References

[1] Sharma, R. and Anker, S.D. (2002) Int. J. Cardiol. 85, 161 171.
[2] Argilés, J.M., Alvarez, B. and López-Soriano, F.J. (1997) Medicinal Res. Rev. 17, 477 498.
[3] Turrin, N.P. and Plata-Salamán, C.R. (2000) Brain Res. Bulletin 51, 3 9.
[4] Li, S., Wang, Y., Matsumura, K., Ballou, L.R., Morham, S.G. and Blatteis, C.M. (1999) Brain Res. 825, 86 94.
[5] Porter, M.H., Hrupka, B.J., Altreuther, G., Arnold, M. and Langhans, W. (2000) Am. J. Physiol. Regul. Integr. Comp. Physiol. 279, R2113 R2120.
[6] Coma, M., Vicente, R., Busquets, S., Carbó, N., Tamkun, M.M., López-Soriano, F.J., Argilés, J.M. and Felipe, A. (2003) FEBS Lett. 536, 45 50.
[7] Selmaj, K.W. and Raine, C.S. (1988) Ann. Neurol. 23, 139 346.
[8] Boka, G., Anglade, P., Wallach, D., Javoy-Agid, F., Agid, Y. and Hirsch, E.C. (1994) Neurosci. Lett. 172, 151 154.
[9] Fillit, H., Ding, W.H., Buee, L., Kalman, J., Altstiel L., Lawlor, B. and Wolf-Klein, G. (1991) Neurosci. Lett. 129, 318 320.
[10] Hille, B. (2001) Ion channels of excitable membranes. Sinauer associates Inc, Sunderland, MA.
[11] Houzen, H., Kikuchi, S., Kanno, M., Shinpo, K. and Tashiro, K. (1997) J. Neurosci. Res. 50, 990 999.
[12] Köller, H., Allert, N., Oel, D., Stoll, G. and Siebler, M. (1998) Neuro Report 9, 1375 1378.
[13] Wu, S.N., Lo, Y.K., Kuo, B.I. and Chiang, H.T. (2001) Endocrinology 142, 4785 4794.
[14] Diem, R., Meyer, R., Weishaupt, J.H. and Bahr, M. (2001) J. Neurosci. 21, 2058 2066.
[15] Vicente, R., Escalada, A., Coma, M., Fuster, G., Sanchez-Tillo, E., Lopez-Iglesias, C., Soler, C., Solsona, C., Celada, A. and Felipe, A. (2003) J. Biol. Chem. 278, 46307 46320.
[16] Kupper, J., Prinz, A.A. and Fromberg, P. (2002) Plügers Arch.-Eur. J. Physiol. 443, 541 547.
[17] Horio, Y. (2001) Jpn. J. Pharmacol. 87, 1 6.
[18] Llovera, M., García-Martínez, C., López- Soriano, F.J. and Argilés, J.M. (1994) Biochem. Mol. Biol. Int. 33, 681 689.

194

[19] Bruce, A.J., Boling, W., Kindy, M.S., Peschon, J., Kraemer, P.J., Carpenter, M.K., Holtsberg, F.W. and Mattson, M.P. (1996) Nat. Med. 2, 788 794.

[20] Xaus, J., Comalada, M., Valledor, A.F., Lloberas, J., López-Soriano, F.J., Argilés, J.M., Bogdan, C. and Celada, A. (2000) Blood 95, 3823 3831.

[21] Busquets, S., Alvarez, B., Van Royen, M., Figueras, M.T., López-Soriano, F.J. and Argilés, J.M. (2001) Biochim. Biophys. Acta 1499, 249 256.

[22] Garcia-Martinez, C., Agell, N., Llovera, M., Lopez-Soriano, F.J. and Argiles, J.M. (1993) FEBS Lett. 323, 211 214.

[23] Garcia-Martinez, C., Llovera, M., Agell, N., Lopez-Soriano, F.J. and Argiles, J.M. (1994) Biochem. Biophys. Res. Commun. 201, 682 686.

[24] Busquets, S., Sanchis, D., Alvarez, B., Ricquier, D., Lopez-Soriano, F.J. and Argiles, J.M. (1998) FEBS Lett. 440, 348 350.

[25] Fuster, G., Vicente, R., Coma, M., Grande, M. and Felipe, A. (2002) Methods Find. Exp. Clin. Pharmacol. 24, 253 259.

[26] Grande, M., Suàrez, E., Vicente, R., Cantó, C., Coma, M., Tamkun, M.M., Zorzano, A., Gumà, A. and Felipe, A. (2003) J. Cell. Physiol. 195, 187 193.

[27] Coma, M., Vicente, R., Tsevi, I., Grande, M., Tamkun, M.M. and Felipe, A. (2002) J. Physiol. Biochem. 58, 195 203.

[28] Frost, R.A., Nystrom, G.J. and Lang, C.H. (2003) Endocrinobgy 144, 1770 1779.

[29] Madiehe, A.M., Mitchell, T.D. and Harris, R.B. (2003) Am. J. Physiol. Regul. Integr. Comp. Physiol., R763 R770.

[30] Chung, S., Lee, J., Joe, E.H. and Uhm, D.Y. (2001) Neurosci. Lett. 300, 67 70.

[31] Callewaert, G., Hanbauer, I. and Morad, M. (1989) Science 243, 663 666.

[32] Espinosa, F., McMahon, A., Chan, E., Wang, S., Ho, C.S., Hantz, N. and Joho, R.H. (2001) J. Neurosci. 21, 6657 6665.

[33] Giese, P.K., Storn, J.F., Reuter, D., Fedorov, N.B., Shao, L.-R., Leicher, T., Pongs, O. and Siva, A.J. (1998) Learning and Memory 5, 257 273.

[34] Slotwinski, R., Olszewski, W.L., Chaber, A., Slodkowski M., Zaleska, M. and Krasnodebski, I.W. (2002) J. Clin. Immunol. 22, 289 296.

[35] Muc-Wierzgon, M., Nowakowska-Zajdel, E., Zubelewicz, B., Wierzgon, J., Kokot, T., Klakla, K., Szkilnik, R. and Wiczkowski, A. (2003) J. Exp. Clin. Cancer Res. 22, 171 178.

[36] Sugano, M., Tsuchida, K., Hata, T. and Makino, N. (2004) FASEB. J. 18, 911 913.

[37] Sugano, M., Tsuchida, K. and Makino, N. (2004) Mol. Cell. Biochem. 258, 57 63.

[38] Wesselingh, S.L., Power, C., Glass, J.D., Tyor, W.R., McArthur, J.C., Farber, J.M., Griffin, J.W. and Griffin, D.E. (1993) Ann. Neurol. 33, 576 582.

[39] Eder, C. (1998) Am. J. Physiol. Cell. Physiol. 275, C327 C342.

[40] Draheim, H.J., Prinz, M., Weber, J.R., Weiser, T., Kettenmann, H. and Hanisch, U.K. (1999) Neuroscience 89, 1379 1390.

[41] Nelson, D.J., Jow, B. and Jow, F. (1992) J. Membr. Biol. 125, 207 218.

[42] Lucas, R., Magez, S., De Leys, R., Fransen, L., Scheerlinck, J.P., Rampelberg, M., Sablon, E. and De Baetselier, P. (1994) Science 263, 814 817.

[43] Hribar, M., Bloc, A., van der Goot, F.G., Fransen, L., De Baetselier, P., Grau, G.E., Bluethmann, H., Matthay, M.A., Dunant, Y., Pugin, J. and Lucas, R. (1999) Eur. J. Immunol. 29, 3105 3111.

[44] Soler, C., Valdés, R., García-Manteiga, J., Xaus, J., Comalada, M., Casado, F.J., Modolell, M., Nicholson, B., MacLeod, C., Felipe, A., Celada, A. and Pastor-Anglada, M. (2001) J. Biol. Chem. 276, 30043 30049.

[45] Freitas, J.J.S., Pompéia, C., Miyasaka, C.K. and Curi, R. (2001) J. Neurochem. 77, 655 663.

4.2. Bloque 2

Los cambios electrofisiológicos que se presentan en la corriente de salida de potasio dependiente de voltaje, en proliferación y activación, pueden ser debidos a cambios en la composición del complejo funcional. Con el fin de explorar esta idea se han caracterizado las subunidades Kvμ presentes en estas células y se han realizado estudios sobre la posible asociación entre Kv1.5 y Kv1.3.

La primera contribución de este bloque describe la presencia en macrófagos de todas las subunidades Kvμ estudiadas menos la Kvμ4. La proliferación inducida por MCSF incrementaría la expresión de todas las subunidades auxiliares mientras que distintos estímulos de activación, LPS y TNFμ, regulan la expresión génica de estas proteínas de distinta forma. Los parámetros cinéticos de la corriente de salida de potasio sobre los que estas subunidades actúan, como son las constantes de activación, inactivación y deactivación, han sido analizados en un intento de relacionar cambios moleculares con cambios electrofisiológicos en macrófagos proliferantes y activados.

El segundo apartado de este bloque lo forma una publicación en preparación en la que se describe cómo Kv1.5 es capaz de asociarse con Kv1.3 para formar un complejo funcional generador de corrientes de salida de potasio. En este trabajo se muestran estudios de asociación por microscopia confocal y electrónica junto con estudios de farmacología que confirman la formación del complejo heteromérico. Los cambios en los parámetros electrofisiológicos de las corrientes, dependiendo de la composición del complejo, se han analizado en distintos modelos de expresión heteróloga. Por último se sugiere que, los cambios en el *gating* que se producen en esta corriente ante distintos estímulos, como el TNFμ, podrían deberse a cambios en la estequiometría de las subunidades que conforman el complejo generador de la corriente de salida de potasio en macrófagos.

CONTRIBUCIONES

4.2.1. Pattern of Kv beta subunit expression in macrophages depends upon proliferation and the mode of activation.

4.2.2. Association of Kv1.5 to Kv1.3 contributes to the major voltage dependent K$^+$ channel in macrophages.

Pattern of Kvβ Subunit Expression in Macrophages Depends upon Proliferation and the Mode of Activation[1]

Rubén Vicente,[2]* Artur Escalada,[2‡] Concepció Soler,[†] Maribel Grande,* Antonio Celada,[‡] Michael M. Tamkun,[¶] Carles Solsona,[§] and Antonio Felipe[3]*

Voltage-dependent potassium channels (Kv) in leukocytes are involved in the immune response. In bone marrow-derived macrophages (BMDM), proliferation and activation induce delayed rectifier K$^+$ currents, generated by Kv1.3, via transcriptional, translational, and posttranslational controls. Furthermore, modulatory Kvβ subunits coassociate with Kvα subunits, increasing channel diversity and function. In this study we have identified Kvβ subunits in mouse BMDM, studied their regulation during proliferation and activation, and analyzed K$^+$ current parameters influenced by these proteins. BMDM express all isoforms of *Kvβ1* (Kvβ1.1, Kvβ1.2, and Kvβ1.3) and *Kvβ2* (Kvβ2.1), but not *Kvβ4*, the alternatively spliced murine *Kvβ3* variant. M-CSF-dependent proliferation induced all Kvβ isoforms. However, LPS- and TNF-α-induced activation differentially regulated these subunits. Although LPS increased Kvβ1.3, reduced Kvβ1.2, and maintained Kvβ1.1 mRNA levels constant, TNF-α up-regulated Kvβ1.1, down-regulated Kvβ1.2, and left Kvβ1.3 expression unchanged. Moreover, in contrast to TNF-α, M-CSF- and LPS-up-regulated Kvβ2.1. K$^+$ currents from M-CSF- and LPS-stimulated BMDM exhibited faster inactivation, whereas TNF-α increased τ values. Although in M-CSF-stimulated cells the half-inactivation voltage shifted to more positive potentials, the incubation with LPS and TNF-α resulted in a hyperpolarizing displacement similar to that in resting BMDM. Furthermore, activation time constants of K$^+$ currents and the kinetics of the tail currents were different depending upon the mode of activation. Our results indicate that differential Kvβ expression modifies the electrical properties of Kv in BMDM, dependent upon proliferation and the mode of activation. This could determine physiologically appropriate surface channel complexes, allowing for greater flexibility in the precise regulation of the immune response. *The Journal of Immunology*, 2005, 174: 4736–4744.

The activation and proliferation of cells in the immune system are modulated by membrane transduction of extracellular signals. Some interactions occur via the regulation of transmembrane ion fluxes, and several studies suggest that some signaling occurs through ion movements in macrophages. Changes in the membrane potential are among the earliest events after stimulation of macrophages, and ion channels underlie the Ca^{2+} signal involved in the leukocyte activation (1). Potassium channels indirectly determine the driving force for Ca^{2+} entry (2). The resting membrane potential in leukocytes is about −50 to −60 mV, and these channels serve to hyperpolarize the membrane even further to −80 mV (2). This hyperpolarization accentuates Ca^{2+}

influx to promote Ca^{2+}-dependent signal transduction pathways that depend upon the activity of ion channels (1–4).

Voltage-dependent potassium channels (Kv)[4] play a crucial role in excitable cells by determining resting membrane potential and controlling action potentials (5). In addition, they are involved in the activation and proliferation of leukocytes (1–4). The mammalian Shaker family (Kv1) contains at least eight different genes (Kv1.1 to Kv1.8) that can form functional homo- and heterotetrameric complexes (6). Thus, Kv1 channels can assemble promiscuously, yielding a wide variety of biophysically and pharmacologically distinct channels (5). In addition, assigning specific K$^+$ channel clones to native currents is often difficult, because this complexity is enhanced by the presence of Kvβ regulatory subunits (7). Up to four different forms of these cytoplasmic proteins can form part of the heteromeric structure ($α_4β_n$). Different *Kvβ* genes, namely *Kvβ1*, *Kvβ2*, and *Kvβ3* generate up to six different Kvβ proteins. Although Kvβ1.1, Kvβ1.2, and Kvβ1.3 are alternatively spliced forms from the *Kvβ1* gene, Kvβ2.1 is the only variant known to be generated from the *Kvβ2* gene (7). In addition, *Kvβ3* generates two alternatively spliced isoforms, Kvβ3 and Kvβ4, expressed in rat and mouse brain, respectively (8, 9). All subunits are ~300 aa in length and share a common conserved core (>85% amino acid identity), with the highest degree of variability in the N termini. Their association with the Kvα subunit occurs via the conserved C-terminal end. Furthermore, Kvβ regulatory subunits generally assemble with channels from the Kv1 family (7).

We previously described the expression of Kv1.3 and Kv1.5 in bone marrow-derived macrophages (BMDM) (10). Macrophage

*Molecular Physiology Laboratory, Departament de Bioquímica i Biologia Molecular and †Departament de Fisiologia, Universitat de Barcelona, and ‡Macrophage Biology Group, Biomedical Research Institute of Barcelona, Barcelona, Spain; §Cellular and Molecular Neurobiology Laboratory, Departament de Biologia Cellular i Anatomia Patològica, Universitat de Barcelona Campus de Bellvitge, Hospitalet de Llobregat, Spain; and ¶Departments of Physiology and Biochemistry and Molecular Biology, Colorado State University, Fort Collins, CO 80523

[4] Abbreviations used in this paper: Kv, voltage-dependent potassium channel; BMDM, bone marrow-derived macrophage; MgTx, rMargatoxin.

K$^+$ channels are tightly regulated during M-CSF-dependent proliferation, and LPS- or TNF-α-induced activation and their functional activity are important for cellular responses. Proliferation and activation induce outward K$^+$ currents under transcriptional and translational control. Several lines of evidence led to the conclusion that LPS-induced activation regulates Kv via TNF-α-dependent and -independent mechanisms (10). In addition, our results indicate that posttranslational events are involved in the differential Kv regulation in response to different stimuli (10). Kvβ subunits confer rapid inactivation, alter current amplitude and gating, and promote Kv cell surface expression. In fact, both Kv1.3 and Kv1.5 are able to assemble with Kvβ subunits to form functional Kv channels, increasing the variety of electrical responses (11–13). Nevertheless, only a few studies have been undertaken to identify Kvβ subunits expressed in immune system cells. Thus, F5, an IL-2-induced cDNA in Th lymphocytes, turned out to be the Kvβ2.1 subunit (14). In addition, Kvβ1.1 and Kvβ2.1 subunits are up-regulated during mitogen-stimulated activation of mouse T cells (15). Furthermore, the heterologous expression of Kv1.3 and Kv1.5 together with Kvβ subunits in *Xenopus* oocytes and mammalian cells, respectively, dramatically modifies the rate of inactivation and the amplitude of the K$^+$ current (12, 13).

In this study we describe, for the first time, the expression of Kvβ subunits that may coassemble with Kv1.3 in BMDM to generate different functional Kv channel complexes. Macrophages express all isoforms of *Kvβ1* (Kvβ1.1, -1.2, and -1.3) and *Kvβ2* (Kvβ2.1). In contrast, Kvβ4, the murine isoform of *Kvβ3* was absent. Although M-CSF-dependent proliferation increased the expression of all Kvβ subunits, it was differentially regulated by LPS- and TNF-α-induced activation. Kvβ subunits triggered a finely tuned modulation of macrophage electrical activity dependent upon proliferation and mode of activation. These data suggest that by changing the heteromeric Kv channel structure, macrophages could physiologically set the membrane potential to achieve precise immune responses.

Materials and Methods
Isolation of BMDM and cell culture

BMDM from 6- to 10-wk-old BALB/c mice (Charles River Laboratories) were isolated and cultured as described previously (16). Briefly, animals were killed by cervical dislocation, and both femurs were dissected. The ends of the bones were removed, and the marrow tissue was flushed out by irrigation with DMEM. Once dispersed by passing through a 25-gauge needle, the cells were cultured in plastic dishes (150 mm) in DMEM containing 20% FBS and 30% L cell supernatant of L-929 fibroblast (L cell)-conditioned medium as a source of M-CSF and kept at 37°C in a humidified 5% CO$_2$ atmosphere. Macrophages were obtained as a homogeneous population of adherent cells after 7 days of culture. For experiments, they were cultured with the same tissue culture differentiation medium (DMEM, 20% FBS, and 30% L cell medium) or arrested at G$_0$ by M-CSF deprivation in DMEM supplemented with 10% FBS for at least 18 h (basal). Resting (G$_0$-arrested) cells were further incubated in the absence or the presence of recombinant murine M-CSF (1200 U/ml), with or without LPS (100 ng/ml) or TNF-α (100 ng/ml), for the indicated times. All animal handling was approved by the ethics committee of University of Barcelona in accordance with European Union regulations.

HEK-293 cells that lack expression of Kvβ subunits were used as negative controls and cultured as described previously (17).

RNA isolation and RT-PCR analysis

Total RNA from mouse macrophages, brain, and liver was isolated using the Tripure reagent (Roche), according to the manufacturer's instructions. Samples were also treated with the DNA-free kit from Ambion to remove DNA.

Ready-to-Go RT-PCR Beads (Amersham Biosciences) were used in a one-step RT-PCR as described previously (18). Total RNA and selected primers (1 μM) were added to the beads. The reverse transcription reaction was initiated by incubating the mixture at 42°C for 30 min. Once first-strand cDNA had been synthesized, the conditions were set for additional

PCR: 92°C for 30 s, either 55°C (Kv1.3, Kv1.5, Kvβ1.2, and 18S) or 60°C (rest of Kvβ) for 1 min, and 72°C for 2 min. These settings were applied for 40 cycles. After every 10 cycles, 10 μl of the total reaction were collected in a separate tube for electrophoresis and further analysis. A range of RNA dilutions from each independent sample was performed to obtain an exponential phase of amplicon production (data not shown), as described previously (19). The same independent RNA aliquot was used to analyze mRNA expression and the respective amount of 18S rRNA. In all cases negative controls were performed in the absence of the reverse transcription reaction. Because Kvβ isoforms have a highly homologous core, we designed specific primers to the N terminus for each subunit. Primer sequences, accession numbers, and cDNA lengths are shown in Table I.

Once the exponential phase of amplicon production had been determined the specificity of each product was confirmed in test RT-PCRs using the appropriate cDNA probe in a Southern blot analysis. PCR-generated cDNA probes from mouse brain were subcloned using the pSTBlue-1 acceptor vector kit (Novagen), and the sequences were confirmed using the Big Dye Terminator Cycle Sequencing kit and an ABI 377 sequencer (Applied Biosystems). *EcoRI*-digested [α-^{32}P]CTP random primer-labeled cDNAs were used as probes, as described previously (19). At least three different filters were prepared from independent samples, and representative blots are shown. Results were analyzed with Phoretix software (Nonlinear Dynamics).

Preparation of crude membrane fractions from BMDM and Western blot analysis

Crude membrane preparations were obtained as described previously (20). Macrophages and HEK-393 cells were washed twice in cold PBS and lysed on ice with lysis solution containing 0.32 M sucrose, 5 mM Na$_2$HPO$_4$, and the following protease inhibitors: 0.31 mg/ml benzamidine, 0.62 mg/ml N-ethylmaleimide, 1 mg/ml bacitracin (Sigma-Aldrich), 1 μg/ml pepstatin, 1 μg/ml leupeptin, and 0.07 μg/ml Pefablock (Roche). Brain samples were also homogenized in the same lysis solution in a glass homogenizer. Lysates were centrifuged at 4°C at 3000 rpm for 10 min to remove large debris and nuclei. The supernatant was collected and further centrifuged for 1 h at 4°C at 15,000 rpm. The resulting membrane pellet was resuspended in ice-cold PBS and stored at -80°C. The sample protein concentration was determined by Bio-Rad protein assay. Crude membrane proteins (25 μg) were boiled at 95°C in Laemmli SDS-loading buffer and separated by 10% SDS-PAGE. They were transferred to nitrocellulose membranes (Immobilon-P, Millipore) and blocked in 5% dry milk-supplemented 0.2% Tween 20 PBS before immunoreaction. To monitor Kvβ subunits, the following Abs were donated by Dr. J. Trimmer (University of California, Davis, CA): anti-Kvβ1.1 rabbit polyclonal, anti-Kvβ1.2 rabbit polyclonal, anti-pan Kvβ rabbit polyclonal, and anti-Kvβ2.1 mouse monoclonal (11, 21–23). The anti-Kvβ1.3 rabbit polyclonal Ab was produced and characterized in the Tamkun laboratory (20). An anti-β-actin mAb (Sigma-Aldrich) was used as a loading and transfer control.

Electrophysiological recordings

Whole-cell currents were measured using the patch-clamp technique. An EPC-9 (HEKA) with the appropriate software was used for data recording and analysis. Currents were filtered at 2.9 kHz. Patch electrodes of 2–4 MOhm were produced from borosilicate glass (outer diameter, 1.2 mm; inner diameter, 0.94 mm; Clark Electromedical Instruments) with a P-97 puller (Sutter Instruments). Electrodes were filled with the following solution: 120 mM KCl, 1 mM CaCl$_2$, 2 mM MgCl$_2$, 10 mM HEPES, 11 mM EGTA, and 20 mM D-glucose, adjusted to pH 7.3 with KOH. The extracellular solution contained the following: 120 mM NaCl, 5.4 mM KCl, 2 mM CaCl$_2$, 1 mM MgCl$_2$, 10 mM HEPES, and 25 mM D-glucose, adjusted to pH 7.4 with NaOH. After establishing a whole-cell configuration, macrophages were clamped to a holding potential of -60 mV, with seal resistances of at least 2.5 GOhm. All recordings were routinely subtracted for leak currents online. Only cells with a series resistance compensation of 80–90% were selected for analysis. Uncompensated series resistances were 4–8 MOhm, as currents evoked were <1 nA; voltage errors from uncompensated series resistance were <2 mV.

To evoke voltage-dependent currents, cells were stimulated with specific square pulses ranging from -60 to $+50$ mV in 10-mV steps. Protocols are detailed in the figures.

To pharmacologically characterize the voltage-dependent outward K$^+$ current, rMargatoxin (rMgTx) and ShK-Dap^{22} were added to the external solution (24, 25). Toxins were reconstituted at 10 μM in Tris buffer (0.1%

Table I. *Genes, accession numbers, and sequences of oligonucleotide primers, base pairs, and cDNA length*

Gene	Accession No.	Sequence[a]	Base Pairs	Length (bp)
Kv1.3	M30441	F: 5'-CTCATCTCCATTGTCATCTTCTGA-3'	741-765	
		R: 5'-TTGAATTGGAAACAATCAC-3'	1459-1440	718
Kv1.5	AF302768	F: 5'-GGATCACTCCATCACCAG-3'	3003-3020	
		R: 5'-GGCTTCCTCCTCTTCCTTG-3'	3337-3320	334
Kvβ1.1	X70662	F: 5'ATGCAAGTCTCCATAGCCTGCACA-3'	332-356	
		R: 5'-CTATATTTCATGCCAGTCTGCTTT-3'	552-528	220
Kvβ1.2	L39833	F: 5'-ATGCATCTGTATAAACCTGCCTGT-3'	89-113	
		R: 5'-CTGTATGCCATGCCCGTCTCTGCT-3'	330-306	241
Kvβ1.3	L47665	F: 5'-ATGCTGGCAGCCCGGACAGGGGCA-3'	54-78	
		R: 5'-CTGTGCGGCATGCCTGTGGTGCAG-3'	328-304	274
Kvβ2.1	L48983	F: 5'-CAGGATTCCCCCTCTGTGAAAAGG-3'	138-162	
		R: 5'-CTGTAAAACTGGAGCTGTCTTTTG-3'	317-292	179
Kvβ4	U65593	F: 5'-ATGTCAAGAGGGTATGGTCTGATA-3'	1-24	
		R: 5'-TAGGTCATGGCTCTCACAATCTCC-3'	182-159	182
18S	X00686	F: 5'-CGCAGAATTCCCACTCCCGACCC-3'	482-498	
		R: 5'-CCCAAGCTCCAACTACGAGC-3'	694-675	212

[a] F, forward; R, reverse.

BSA, 100 mM NaCl, and 10 mM Tris, pH 7.5). All recordings were performed at room temperature (20–23°C).

Analysis and statistics

According to the solutions used, the calculated equilibrium potential for potassium was −79 mV (E_K) using the Nernst equation. The normalized G/G_{max} vs the voltage curve was fitted using Boltzmann's equation: $G/G_{max} = 1/(1 + \exp((V_{1a} - V/k))$, where V_{1a} is the voltage at which the current is half-activated, and k is the slope factor of the activation curve.

Steady-state inactivation plots were fitted to a Boltzmann equation as follows: $I/I_{max} = 1/(1 - \exp((V_{1/2} - V/k))$.

Activation, inactivation, and deactivation time constants were adjusted to single exponential functions: $I(t) = A(1 - \exp(-t/\tau))$ for activation τ, calculated from the end of the compensated capacitive transient to the peak of the current and $I(t) = A\exp(-t/\tau)$ for inactivation and deactivation τ. Inactivation adjustment was calculated from the peak of the current to the

steady-state inactivation, and deactivation was fitted from the peak of the tail current to steady state; traces were fitted with SigmaPlot (SPSS).

Values are expressed as the mean ± SEM. The significance of the differences was established either by Student's *t* test or one-way ANOVA (PRISM 3.0, GraphPad) for either two-group or two-factor comparisons, respectively. Where indicated, a Tukey post hoc test was performed. A value of $p < 0.05$ was considered significant.

Reagents

Recombinant murine TNF-α was obtained from PeproTech EC; recombinant murine M-CSF was purchased from R&D Systems; LPS was purchased from Sigma-Aldrich; rMgTx was obtained from Alomone Laboratories; ShK-Dap[22] was purchased from Bachem; other reagents were of analytical grade.

FIGURE 1. M-CSF, LPS, and TNF-α increase delayed rectifier K⁺ currents generated by Kv1.3 in macrophages. *A*, Representative traces of delayed rectifier K⁺ currents. Resting cells were incubated for 24 h in the absence (basal) or the presence of M-CSF, with or without LPS or TNF-α. Outward traces were elicited by a depolarizing step as indicated. *B*, Steady-state activation curves. Cells were held at −60 mV, and pulse potentials were applied from −60 to +50 mV in 10-mV steps of 200 ms. Conductances were normalized to the peak current density at +50 mV. ○, basal; ●, M-CSF; □, LPS; ■, TNF-α. *C*, Macrophages express Kv1.3 and Kv1.5. One microgram of total RNA from mouse brain, macrophages, and liver was used in RT-PCRs as described in *Materials and Methods*. *D*, Inhibition of K⁺ currents by MgTx and ShK-Dap[22]. Currents were elicited in BMDM as described in *A*. The percentage of peak current was calculated by comparing the current at a given concentration of toxin vs that obtained in its absence. Concentrations of 50 and 500 pM toxin were selected to block the peak current either partially (~50%) or totally (~100%), respectively. ■, MgTx; □, ShK-Dap[22].

The Journal of Immunology   4739
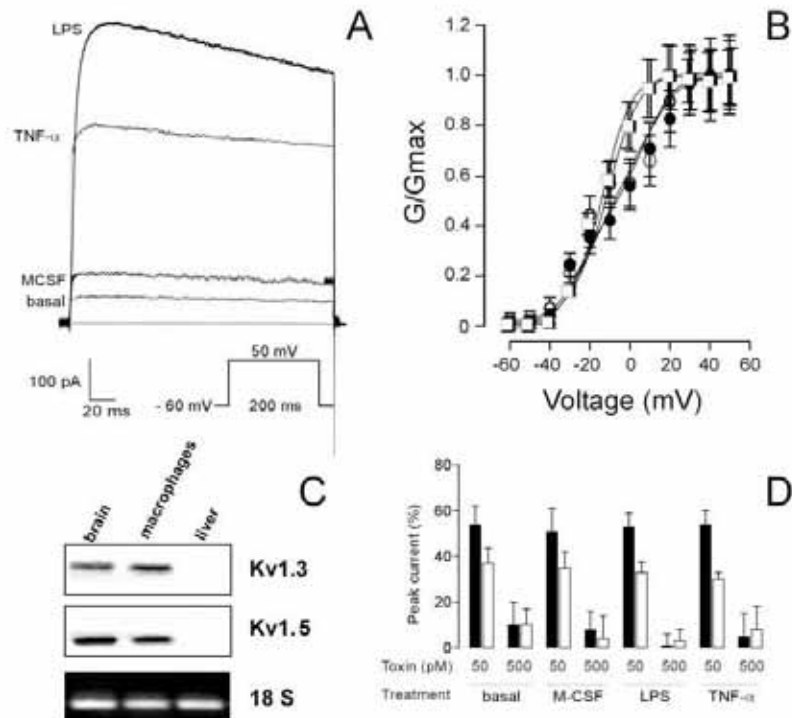
Results

Delayed rectifier K^+ currents were evoked in BMDM by depolarizing pulses (Fig. 1A) as described previously (10). Resting macrophages ($n = 40$) exhibited an outward conductance with ~40 pA peak current amplitude. M-CSF enhanced K^+ currents ~2-fold (~90 pA; $n = 120$). Both LPS and TNF-α further increased the current amplitude (~600 and ~350 pA, respectively; $n = 60$). Resting and M-CSF-treated BMDM showed similar voltage dependence (Fig. 1B). Channels opened at depolarizing potentials (−40 to −30 mV) with $V_{1/2}$ values of −12.2 ± 1.3 and −12.4 ± 2.1 mV and k slopes of 20.5 ± 2.5 and 22.0 ± 3.0 mV for resting and M-CSF-treated macrophages, respectively ($n = 30$). Macrophages incubated with LPS and TNF-α were activated (10), and the steady-state activation curve of normalized conductances changed substantially (Fig. 1B). Although channels were open at the same depolarizing pulse potentials with $V_{1/2}$ values similar to those observed with M-CSF (−14.3 ± 3.4 and −15.1 ± 3.1 mV for LPS and TNF-α, respectively; $n = 12$), k slope values were significantly different (9.6 ± 1.6 and 9.1 ± 2.2 mV for LPS and TNF-α, respectively; $p < 0.001$ vs M-CSF, by Student's t test; $n = 12$). RT-PCR experiments (Fig. 1C) showed that Kv1.3 and Kv1.5 mRNAs are present in brain and BMDM but not in liver. Moreover, the MgTx- and ShK-Dap[22]-mediated inhibition of K^+ currents evoked in response to different stimuli (Fig. 1D) suggested that outward conductances were principally mediated by Kv1.3, as demonstrated previously (10).

The oligomeric structure of the Kv complex is a critical determinant of electrical activity in mammalian neurons (26). Because modulation by accessory β subunits has dramatic consequences on Kv1 functional activities (7), we studied the expression of Kvβ proteins in crude membrane preparations using several specific Abs. Unfortunately, none of the anti-Kvβ1 subunit-specific Abs produced a reliable signal (data not shown). Only the polyclonal anti-pan-β subunit and the monoclonal anti-Kvβ2.1 were useful in our BMDM samples. In macrophages, the anti-pan-β subunit Ab recognizes two polypeptide species of ~38 and ~41 kDa, similar to those described by Trimmer and collegues (11, 22) in the brain. Kvβ2.1 protein corresponds to the lower band, and the higher band corresponds to Kvβ1 peptides sharing a common core (Fig. 2A). HEK-293 cells were negative. Although M-CSF and LPS induced

Kvβ1 and Kvβ2.1 expression in macrophages, TNF-α did not. The anti-Kvβ2.1 mAb gave similar results (data not shown).

To further determine Kvβ expression in BMDM, we designed oligonucleotides to amplify the N-terminal domain for each subunit and generated specific Kvβ cDNA probes (Table I). To control for undesirable cross-hybridizations, each Kvβ fragment was run on a 2% agarose gel and further hybridized against the rest of the Kvβ cDNAs. No signal was detected other than that expected with the appropriate specific Kvβ probe (data not shown). Fig. 2B demonstrates that BMDM expressed several Kvβ isoforms similar to the brain. All splice variants of the *Kvβ1* gene (Kvβ1.1, Kvβ1.2, and Kvβ1.3) were detected, as well as the only *Kvβ2* gene product described to date, Kvβ2.1. In contrast, the murine isoform Kvβ4, identified in brain as a spliced mRNA from *Kvβ3*, was absent in BMDM. Liver was used as a negative control.

The addition of M-CSF to resting macrophages triggers cell growth (10, 16), and under these conditions the expression of Kvβ subunits was induced (Fig. 3A). The three splice variants of the *Kvβ1* gene (Kvβ1.1, Kvβ1.2, and Kvβ1.3) followed the same pattern, with similar values. Thus, the expression peaked after 6 h (~3-fold induction), and remained high throughout treatment ($p < 0.001$, by ANOVA). In contrast, Kvβ2.1 increased steadily throughout the study, and the level of induction after 24 h of incubation was ~5-fold ($p < 0.001$, by ANOVA).

When Kvβ subunits are coexpressed heterologously with Kvα, proteins modulate the inactivation properties of Kv (7). The K^+ current inactivation time constants from BMDM incubated with M-CSF were slightly lower than those in its absence, but showed similar voltage dependence (Fig. 3B). The normalized steady-state inactivation indicated that incubation with the growth factor resulted in a 10-mV positive displacement in the $V_{1/2}$ (−19.6 ± 0.6 and −10.0 ± 0.8 mV for without M-CSF and with M-CSF, respectively; $p < 0.001$, by Student's t test) without changes in the k slope (−6.0 ± 0.7 and −6.9 ± 1.0 mV for without M-CSF and with M-CSF, respectively).

LPS and TNF-α activate macrophages, leading to cell growth arrest (10, 27). LPS-induced activation differentially regulated Kvβ subunits in BMDM (Fig. 4A). Under these conditions, the three splice variants of the *Kvβ1* gene showed different expression

FIGURE 2. Macrophages express Kvβ subunits. A, Protein expression of Kvβ subunits in response to different stimuli in BMDM. Crude membrane samples were obtained from mouse brain, HEK-293 cells, and BMDM as described in *Materials and Methods*. Brain and HEK samples were used as positive and negative controls, respectively. Expression of β-actin was used as a loading control. Representative Western blot analyses are shown in the *upper panels*. *Lower panels*, The densitometric analysis of the data. Values expressed as arbitrary units are the mean ± SEM of three independent experiments. B, Kvβ subunit mRNA expression in brain, macrophages, and liver from mouse. One-step RT-PCR was performed on 1 μg of total RNA, and amplicons were electrophoresed and analyzed as described in *Materials and Methods*. Representative filters are shown.
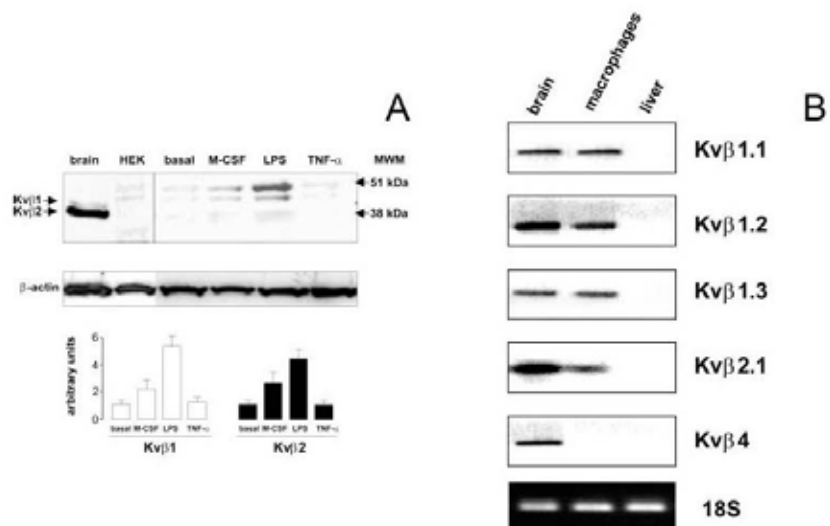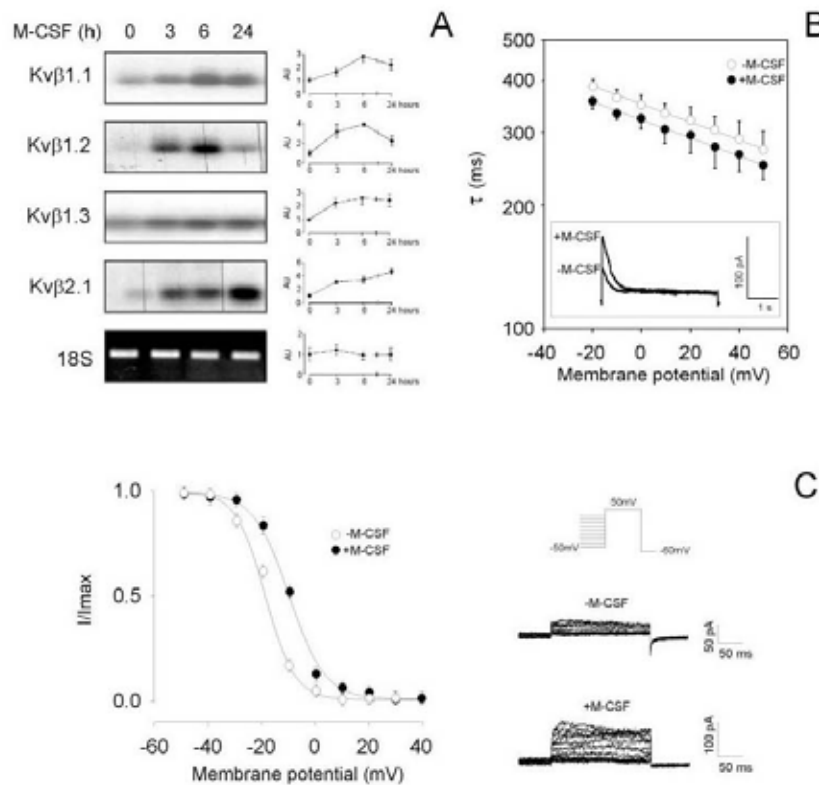
FIGURE 3. M-CSF induces Kvβ subunit mRNA expression and modulates K⁺ current inactivation kinetics in macrophages. *A*, M-CSF induces Kvβ subunit mRNA in macrophages. One-step RT-PCR was performed and analyzed as described in *Materials and Methods*. Samples were collected at different times after the addition of M-CSF. Total RNA concentration and PCR cycles were as follows: Kvβ1.1 and Kvβ1.2, 1 μg and 40 cycles; Kvβ1.3, 0.1 μg and 30 cycles; Kvβ2.1, 0.5 μg and 20 cycles; and 18S, 0.1 μg and 10 cycles. These conditions represent the exponential phase of amplicon production. Representative filters are shown. Values expressed as arbitrary units (AU) are the mean ± SEM of four independent experiments. Significant differences were found with Kvβ1.1, Kvβ1.2, Kvβ1.3, and Kvβ2.1 ($p < 0.001$, by ANOVA). *B*, Plot of inactivation time constant vs test potential. Cells were incubated for 24 h in the presence (●) or the absence (○) of M-CSF. Macrophages were held at −60 mV, and pulse potentials were applied from −60 to +50 mV in 10-mV steps of 4 s. The *inset* illustrates current traces at +50 mV for comparison. *C*, Steady-state inactivation levels of K⁺ currents in the presence (●) or the absence (○) of M-CSF. Cells were treated as described in *B*. Pulse protocols and current traces for both situations are depicted on the *right*. Currents were measured by varying the holding potential from −50 to 40 mV over 4 s, then applying a 200-ms test pulse to 50 mV. To ensure complete recovery from inactivation, cells were repolarized for 45 s at −60 mV. Values are the mean ± SEM of at least four independent cells.

patterns. Although Kvβ1.1 mRNA remained almost constant throughout the study (not significant by ANOVA), both an additional Tukey post hoc test and Student's *t* test indicated that Kvβ1.1 levels were statistically higher at 6 h of incubation (1.0 ± 0.1 vs 1.7 ± 0.2 for 0 and 6 h, respectively; $p < 0.05$; $n = 4$). Kvβ1.2 expression decreased during endotoxin treatment ($p < 0.001$, by ANOVA). In contrast, soon after LPS incubation, Kvβ1.3 mRNA increased ($p < 0.001$, by ANOVA). In addition, Kvβ2.1 mRNA increased steadily throughout the study ($p < 0.001$, by ANOVA). Inactivation of K⁺ currents in macrophages incubated with or without LPS showed similar voltage dependence (Fig. 4*B*). However, the presence of the endotoxin further decreased τ inactivation values. Fig. 4*C* shows that in LPS-treated cells, the half-inactivation voltage shifted in the negative direction by 10 mV, similar to that obtained with nonproliferating BMDM (−10.0 ± 1 and −22.0 ± 1 mV for without LPS and with LPS, respectively; $p < 0.01$, by Student's *t* test) without changes in *k* slope (−6.9 ± 1.0 and −6.6 ± 0.9 mV for without LPS and with LPS, respectively).

Several lines of evidence indicate that LPS exerts Kv regulation via TNF-α-dependent and -independent mechanisms (10, 28). Therefore, we analyzed the effects of TNF-α on the expression of Kvβ subunits (Fig. 5*A*). TNF-α induced an up-regulation of Kvβ1.1 mRNA ($p < 0.001$, by ANOVA), Kvβ1.2 expression decreased steadily throughout the study ($p < 0.001$, by ANOVA), and Kvβ1.3 and Kvβ2.1 remained constant. These results indicate that in contrast to Kv1.3 and other plasma membrane proteins (10, 27, 28), LPS-mediated Kvβ subunit regulation is TNF-α independent in BMDM. Inactivation time constants of K⁺ currents evoked in macrophages incubated with TNF-α were higher than those in its absence, with a significant change in the pattern (Fig. 5*B*). The half-inactivation voltage in TNF-α-stimulated cells shifted to negative potentials, similar to those obtained with nonproliferating macrophages in the absence of M-CSF (see above). Thus, $V_{1/2}$ values were −10.0 ± 1 and −22.2 ± 1 mV for without TNF-α and with TNF-α respectively ($p < 0.001$, by Student's *t* test), and *k* values were −6.9 ± 1.0 and −7.0 ± 1.0 mV for without TNF-α and with TNF-α, respectively (Fig. 5*C*).
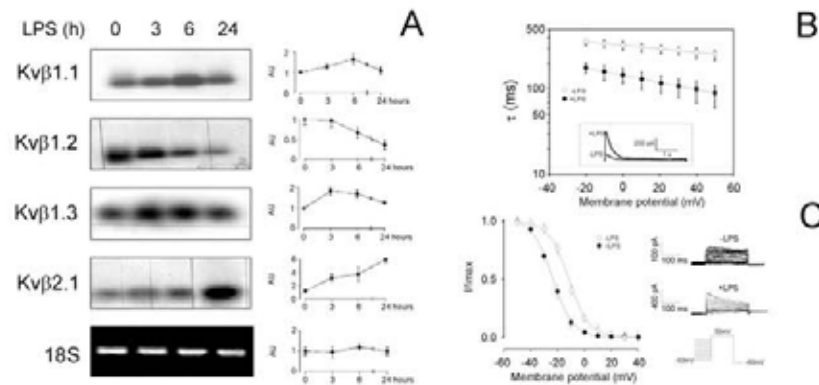
FIGURE 4. Differential regulation of Kvβ isoforms and functional analysis of K$^+$ current inactivation in LPS-treated macrophages. A, BMDM incubated with M-CSF were treated with LPS, and RNA samples were collected at different times before RT-PCR analysis, performed as described in *Materials and Methods*. Total RNA concentration and PCR cycles were as follows: Kvβ1.1 and Kvβ1.2, 1 μg and 40 cycles; Kvβ1.3, 0.1 μg and 30 cycles; Kvβ2.1, 0.5 μg and 20 cycles; and 18S, 0.1 μg and 10 cycles. These conditions represent the exponential phase of amplicon production. Representative filters are shown. Arbitrary unit (AU) values are the mean ± SEM of four independent experiments. Significant differences were found with Kvβ1.2, Kvβ1.3, and Kvβ2.1 ($p < 0.001$, by ANOVA) and Kvβ1.1 at 6 h vs 0 h ($p < 0.05$, by Student's *t* test and ANOVA plus Tukey post hoc test). B, Plot of inactivation time constant vs test potential. Macrophages were incubated with M-CSF for 24 h in the presence (●) or the absence (○) of LPS. Cells were held at −60 mV, and pulse potentials were applied from −60 to +50 mV in 10-mV steps of 4 s. The *inset* illustrates current traces at +50 mV for comparison. C, Steady-state inactivation levels of K$^+$ currents in the presence (●) or the absence (○) of LPS. Cells were treated as described in B. Pulse protocols and current traces for both situations are depicted on the *right*. Currents were measured by varying the holding potential from −50 to 40 mV over 4 s, then applying a 200-ms test pulse to 50 mV. To ensure complete recovery from inactivation, cells were repolarized for 45 s at −60 mV. Values are the mean ± SEM of at least four independent cells.

In addition to inactivation, accessory Kvβ subunits modulate K$^+$ current kinetics by altering activation and deactivation time constants (7). Activation time constants showed voltage dependence (Fig. 6, A–E). However, although LPS exhibited a voltage dependence similar to that obtained with resting and M-CSF-treated macrophages, TNF-α increased τ values at negative potentials (−20 to 0 mV; $p < 0.05$ vs M-CSF, by ANOVA Tukey post hoc

test and Student's *t* test; $n = 4$; Fig. 6A). Analysis of the deactivation time constant was performed as a function of the presence of a tail current. Tail currents were only apparent when cells were treated with activating agents, but not in resting or proliferating macrophages (Fig. 6, F–H). Deactivation time constants (Fig. 6F) and normalized tail currents obtained upon repolarization from +50 to −50 mV (Fig. 6G), indicated that K$^+$ currents deactivated
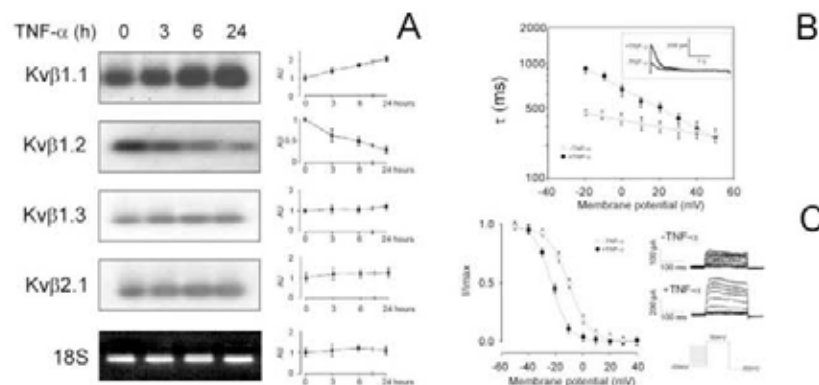

FIGURE 5. TNF-α differentially regulates Kvβ subunit mRNAs and alters the biophysical properties of K$^+$ current inactivation. A, BMDM incubated with M-CSF were treated with TNF-α, and RNA samples were collected at different times before RT-PCR analysis, performed as described in *Materials and Methods*. Total RNA concentration and PCR cycles were as follows: Kvβ1.1 and Kvβ1.2, 1 μg and 40 cycles; Kvβ1.3, 0.1 μg and 30 cycles; Kvβ2.1, 0.5 μg and 20 cycles; and 18S, 0.1 μg and 10 cycles. These conditions represent the exponential phase of amplicon production. Representative filters are shown. Values are the mean ± SEM of four independent experiments. Significant differences were found with Kvβ1.1 and Kvβ1.2 ($p < 0.001$, by ANOVA). B, Plot of inactivation time constant vs test potential. Macrophages were incubated with M-CSF for 24 h in the presence (●) or the absence (○) of TNF-α. Cells were held at −60 mV, and pulse potentials were applied from −60 to +50 mV in 10-mV steps of 4 s. The *inset* illustrates current traces at +50 mV for comparison. C, Steady-state inactivation levels of K$^+$ currents in the presence (●) or the absence (○) of TNF-α. Cells were treated as described in B. Pulse protocols and current traces for both situations are depicted on the *right*. Currents were measured by varying the holding potential from −50 to 40 mV over 4 s, then applying a 200-ms test pulse to 50 mV. To ensure complete recovery from inactivation, cells were repolarized for 45 s at −60 mV. Values are the mean ± SEM of at least four independent cells.
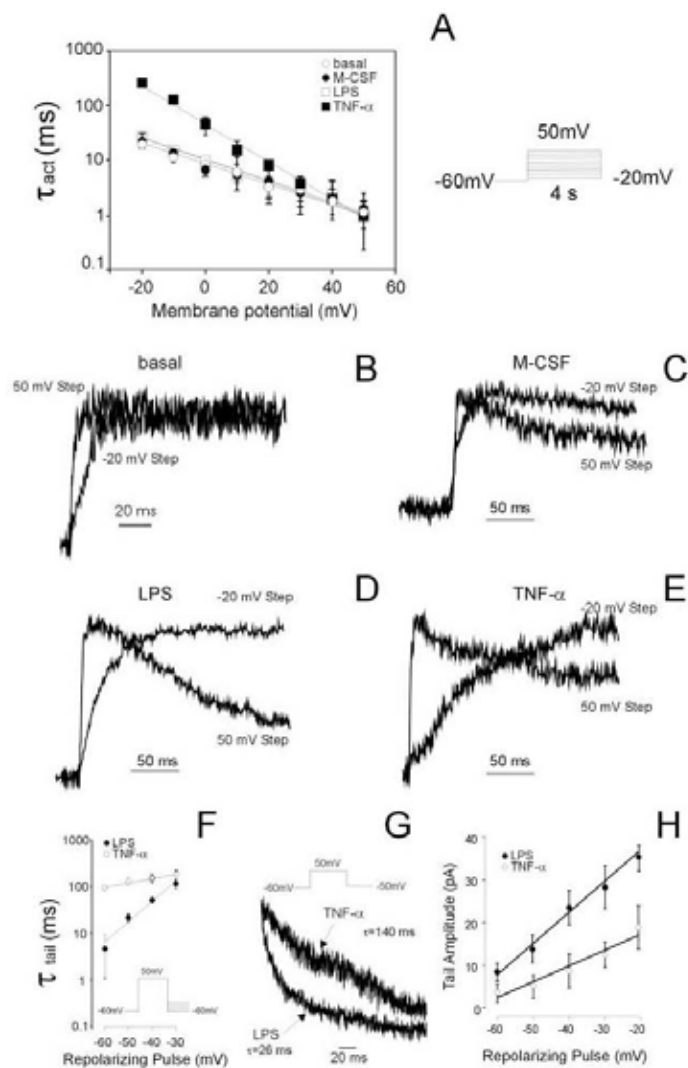
FIGURE 6. Functional analysis of activation and deactivation kinetics in BMDM in response to different stimuli. Macrophages were cultured in the absence of M-CSF for 18 h, then G_0-arrested cells were further incubated for 24 h in the absence (basal) or the presence of M-CSF, with or without LPS and TNF-α. *A,* Voltage dependence of the activation time constant in BMDM. Currents were evoked as described. *B–E,* Representative families of currents at −20 and 50 mV. Traces have been normalized for detail. *F,* Plot of deactivation time constant vs repolarizing pulses in BMDM incubated for 24 h with M-CSF in the presence of LPS (●) and TNF-α (○). Cells were held at −60 mV over 5 s, and a 50-mV pulse of 200 ms was applied, then stepped from −60 to −30 mV over 1 s. *G,* Representative normalized tail currents obtained upon repolarization from +50 to −50 mV in the presence of LPS and TNF-α. Note that the deactivation is slower in the presence of TNF-α (τ = 140 ms) compared with LPS (τ = 26 ms). *H,* Tail current amplitude vs repolarizing pulse in BMDM treated with LPS (●) and TNF-α (○). Pulse protocols are described in *F.* Values are the mean ± SEM of at least four independent cells.

faster in LPS-activated BMDM (τ = 26 ms) than in TNF-α-stimulated cells (τ = 140 ms). Furthermore, tail current amplitudes were significantly different upon the mode of activation (Fig. 6*H*).

Discussion

Proliferation and activation regulate Kv expression in macrophages via transcriptional, translational, and posttranslational controls (10). The outward K^+ current is mainly generated by Kv1.3. However, similar to brain macrophages, a role for Kv1.5 should not be discounted in BMDM. In fact, we observed that K^+ current kinetics in macrophages are significantly different from those described in T cells and heterologous expression systems. Activation and inactivation of Kv1.5 exhibit more depolarized potentials than Kv1.3 currents (29). Heteromeric formation of K^+ channels has been appreciated as a mechanism to increase channel functional diversity, and hybrid channels show a mixture of characteristics of homomeric subunits. Because Kv1.3 and Kv1.5 assemble in macrophages (R. Vicente and A. Felipe, unpublished observations), Kv1.3/Kv1.5 heterotetramers may explain these discrepancies.

We report, for the first time, that macrophages express Kvβ subunits from *Kvβ1* and *Kvβ2*, but not *Kvβ3*. This expression is similar to that in muscle, but different from that in neural tissues, because Kvβ3 and Kvβ4 have only been described in brain (8, 9, 19). This represents another mechanism for regulating K^+ current diversity in BMDM. M-CSF-dependent proliferation does not modify steady-state activation kinetics, but increases current amplitude concomitant with an up-regulation of all Kvβ subunits. However, LPS and TNF-α, which further increased current amplitude, reduced the *k* slope factor. This could be in agreement with changes in gating (30, 31). The expression level, gating, and conductance properties of expressed channels are profoundly influenced by the presence of auxiliary subunits (7, 17, 30, 31). Coexpression of Kvβ1.1 and Kvβ1.2 accelerate the rate of inactivation of K^+ currents arising from Kv1 channels (32–34). However, Kvβ2 exhibits little modulation of fast inactivation and mostly facilitates surface expression (7, 35). The degree of channel inactivation correlates with the charge density of the N terminus of Kvβ1 subunits (34). In this context, it is surprising that, in contrast

to M-CSF-dependent proliferation, *Kvβ1* gene products are clearly differentially regulated in BMDM upon the mode of activation. Thus, distinct Kvβ1 N-terminal domains could be responsible for conferring the heterogeneity of the modulatory activity that we observed.

We found that, in contrast to TNF-α, K$^+$ current inactivation in M-CSF- and LPS-stimulated cells showed similar voltage dependence. However, although resting and M-CSF-treated macrophages exhibit inactivation time constants of between 250 and 400 ms at positive potentials, Kv1.3 currents in LPS-stimulated cells clearly inactivate much faster ($\tau = 100–200$ ms). Kv1.3 expressed in HEK 293 cells, in the absence of Kvβ subunits, inactivates much more slowly ($\tau = 1800$ ms at $+40$ mV) (36). In contrast, in T lymphocytes, which express Kvβ proteins (15), Kv1.3 inactivates with a time constant of 150–200 ms at $+40$mV (37), similar to that in LPS-stimulated BMDM. However, this could be as a result of the model because human T cells were activated with PHA A to increase K$^+$ channel expression (37, 38). Thus, Kv1.3 in BMDM and T cells inactivates faster than in HEK cells, suggesting a role for Kvβ subunits in the leukocyte membrane excitability. In addition, Kv currents in M-CSF-stimulated cells exhibited a shift in $V_{1/2}$ inactivation to more positive potentials, but upon activation, values returned to more negative potentials, which are characteristic of K$^+$ currents in nonproliferating cells.

Macrophage activation also led to important modifications in K$^+$ current activation kinetics and tail currents. These parameters indicated enormous differences between proliferation and the mode of activation and are in agreement with the cell growth arrest triggered by LPS and TNF-α (10, 27). Our results are in agreement with those described when Kv1 proteins are coexpressed with individual Kvβ subunits in heterologous systems (32–35, 39, 40). A possible interpretation, taking into account the fact that M-CSF and LPS both induce Kvβ2.1, is that Kvβ2.1 inhibits Kvβ1-mediated inactivation and promotes Kv surface expression (35, 41, 42). In fact, Kvβ2 subunits self-associate, presumably forming a tetramer (43). This suggests that in the presence of M-CSF and LPS, the heteromeric structure of the channel may contain mainly Kvβ2.1 subunits. This structure would highlight the complex scenario in which the insertion of Kvβ2.1 could change the electrical properties of the Kv channel, leading to multiple physiological effects on the mode of activation.

$\alpha\beta$ interactions may be additionally influenced by differential posttranslational modifications. Kvβ subunits are oxidoreductases that are under oxidative stress and protein kinase regulation (7, 30, 44). In contrast to that by M-CSF, LPS and TNF-α regulation activates different signal transduction pathways involving Ser/Thr protein kinases (45–47). In this context, the inactivation conferred on Kv1.3 by Kvβ1 could be modulated not only by α subunit phosphorylation, but also by phosphorylation of the β subunit itself, which is known to regulate β-mediated effects (7). Thus, in the Kvβ-negative HEK-293 cell line, Kv1.3 sensitivity to protein kinase C and protein kinase A is significantly reduced, in contrast to observations in Jurkat T cells (36). Moreover, protein kinase C is required for Kvβ1.3 effects on Kv1.5 (48), and protein kinase A reduces Kvβ1.3-induced activation of Kv1.5 (49). This is in agreement with our data in which LPS, but not TNF-α, induced Kvβ1.3 and decreased the inactivation time constant. Furthermore, LPS induced Kvβ2.1 in BMDM, and in fibroblasts the presence of this regulatory subunit resulted in a hyperpolarizing displacement of the normalized inactivation curve similar to that we observed in macrophages (17). Moreover, high levels of phosphorylation and Kvβ2.1 up-regulation could trigger inhibition of the Kvβ1-induced inactivation, increasing current amplitudes. In addition, Kvβ1.2-mediated inactivation is not altered by protein kinase A activation

(48), and macrophage activation by LPS and TNF-α triggered a notable decrease in Kvβ1.2 levels. In fact, this could be related to the decrease in peak current amplitudes of Kv1 subunits in whole-cell and macropatch recordings in the presence of Kvβ1.2 (31, 34, 49).

As mentioned above, the cellular redox state represents another important level of Kv posttranslational control. It has been demonstrated that Kvβ oxidoreductase activity and the biophysics of Kvβ inactivating activity are coupled (32). LPS and TNF-α, but not M-CSF, trigger NO production in BMDM through the inducible NO synthase (10). However, the endotoxin is the most powerful NO-stimulating agent (50). High intracellular concentrations of NO would increase the oxidative stress of BMDM, thereby contributing to the pathogenesis of septic shock (51). Thus, an increase in oxidative stress generated by LPS and, to a lesser extent, TNF-α could modulate Kvβ activity, leading to a precise Kv functional role. In this context, treatment of macrophages with the antioxidant *N*-acetylcysteine improves the immune response (52). Furthermore, although Kvβ1.2 and Kvβ1.1 are sensitive to the redox state, Kvβ1.3 is not (30, 34, 49). Such differential sensitivity of Kvβ subunits to the redox state may be important in some pathophysiological conditions, such as ischemia and endotoxic shock. With an abnormal increase in cellular oxygen radicals, the effects of Kvβ1.2 and Kvβ1.1 would be lost, whereas Kvβ1.3 could still modulate Kv1 currents (34). These results suggest important changes in the functional activity of the Kv complex, because although M-CSF and LPS induce Kvβ1.3 expression, TNF-α does not. In addition, it is intriguing that both the growth factor and the endotoxin exhibit similar inactivation behaviors and show an increase in Kvβ2.1 subunit expression. We suggest that different Kvβ subunits extend the range of Kv1.3 modulation and may provide a variable mechanism for adjusting K$^+$ currents in response to alterations in cellular conditions.

In summary, Kv channels are important in BMDM, where they contribute to diverse processes, such as proliferation and activation. We have described, for the first time, the characterization of Kvβ expressed in BMDM and studied their regulation. Stoichiometry may ultimately serve as a key determinant in shaping the repertoire of the Kv1 channels present in the plasma membrane of leukocytes. These data will be critical for further determination of the molecular composition of individual Kv currents and the physiological relevance of these $\alpha\beta$ interactions. Investigation of the mechanisms involved in the regulation of potassium ion conduction is, therefore, essential for the understanding of potassium channel functions in the immune response to infection and inflammation.

Disclosures

The authors have no financial conflict of interest.

References

1. Lewis, R. S., and M. D. Cahalan. 1995. Potassium and calcium channels in lymphocytes. *Annu. Rev. Immunol.* 13:623.
2. Cahalan, M. D., and K. G. Chandy. 1997. Ion channels in the immune system as targets for immunosuppression. *Curr. Opin. Biotech.* 8:749.
3. Gallin, E. K. 1991. Ion channels in leukocytes. *Physiol. Rev.* 71:775.
4. Panyi, G., Z. Varga, and R. Gáspár. 2004. Ion channels and lymphocyte activation. *Immunol. Lett.* 92:55.
5. Hille, B. 2001. *Ion Channels of Excitable Membranes*, 3rd Ed. Sinauer Associates, Sunderland.
6. Gutman, G. A., K. G. Chandy, J. P. Adelman, J. Aiyar, D. A. Bayliss, D. E. Clapham, M. Covarrubias, G. V. Desir, K. Furuichi, B. Ganetzky, et al. 2003. International Union of Pharmacology. XLI. Compendium of voltage-gated ion channels: potassium channels. *Pharmacol. Rev.* 55:583.

7. Martens, J. R., Y. G. Kwak, and M. M. Tamkun. 1999. Modulation of Kv channel α/β subunit interactions. *Trends Cardiovasc. Med.* 9:253.

8. Leicher, T., R. Bahring, D. Isbrandt, and O. Pongs. 1998. Coexpression of the KCNA3B gene product with Kv1.5 leads to a novel A-type potassium channel. *J. Biol. Chem.* 273:35095.

9. Fink, M., F. Duprat, F. Lesage, C. Heurteaux, G. Romey, J. Barhanin, and M. Lazdunski. 1996. A new K⁺ channel β subunit to specifically enhance Kv2.2 (CDRK) expression. *J. Biol. Chem.* 271:26341.

10. Vicente, R., A. Escalada, M. Coma, G. Fuster, E. Sanchez-Tillo, C. Lopez-Iglesias, C. Soler, C. Solsona, A. Celada, and A. Felipe. 2003. Differential voltage-dependent K⁺ channel responses during proliferation and activation in macrophages. *J. Biol. Chem.* 278:46307.

11. Nakahira, K., G. Shi, K. J. Rhodes, and J. S. Trimmer. 1996. Selective interaction of voltage-gated K⁺ channel β-subunits with α-subunits. *J. Biol. Chem.* 271:7084.

12. Sewing, S., J. Roeper, and O. Pongs. 1996. Kvβ 1 subunit binding specific for shaker-related potassium channel α subunits. *Neuron* 16:455.

13. McCormack, T., K. McCormack, M.S. Nadal, E. Vieira, A. Ozaita, and B. Rudy. 1999. The effects of Shaker β-subunits on the human lymphocyte K⁺ channel Kv1.3. *J. Biol. Chem.* 274:20123.

14. Sabath, D. E., P. L. Podolin, P. G. Comber, and M. B. Prystowsky. 1990. cDNA cloning and characterization of interleukin 2-induced genes in a cloned T helper lymphocyte. *J. Biol. Chem.* 265:12671.

15. Autieri, M. V., S. M. Belkowski, C. S. Constantinescu, J. A. Cohen, and M. B. Prystowsky. 1997. Lymphocyte-specific inducible expression of potassium channel β subunits. *J. Neuroimmunol.* 77:8.

16. Soler, C., I. Garcia-Manteiga, R. Valdés, J. Xaus, M. Comalada, F. J. Casado, M. Pastor-Anglada, A. Celada, and A. Felipe. 2001. Macrophages require different nucleoside transport systems for proliferation and activation. *FASEB J.* 15:1979.

17. Uebele, V. N., S. K. England, A. Chaudhary, M. M. Tamkun, and D. J. Snyders. 1996. Functional differences in Kv1.5 currents expressed in mammalian cell lines are due to the presence of endogenous Kvβ 2.1 subunits. *J. Biol. Chem.* 271:2406.

18. Fuster, G., R. Vicente, M. Coma, M. Grande, and A. Felipe. 2002. One-step reverse transcription polymerase chain reaction for semiquantitative analysis of mRNA expression. *Methods Find. Exp. Clin. Pharmacol.* 24:253.

19. Grande, M., E. Suárez, R. Vicente, C. Cantó, M. Coma, M. M. Tamkun, A. Zorzano, A. Gumá, and A. Felipe. 2003. Voltage-dependent K⁺ channel β subunits in muscle: differential regulation during postnatal development and myogenesis. *J. Cell. Physiol.* 195:187.

20. Coppock, E. A., and M. M. Tamkun. 2001 Differential expression of Kv channel α- and β-subunits in the bovine pulmonary arterial circulation. *Am. J. Physiol.* 281:L1350.

21. Bekele-Arcuri, Z., M. F. Matos, L. Manganas, B. W. Strassle, M. M. Monaghan, K. J. Rhodes, and J. S. Trimmer. 1996. Generation and characterization of subtype-specific monoclonal antibodies to K⁺ channel α- and β-subunit polypeptides. *Neuropharmacology* 35:851.

22. Rhodes, K. J., S. A. Keilbaugh, N. X. Barrezueta, K. L. Lopez, and J. S. Trimmer. 1995. Association and colocalization of K⁺ channel α- and β-subunit polypeptides in rat brain. *J. Neurosci.* 15:5360.

23. Rhodes, K. J., B. W. Strassle, M. M. Monaghan, Z. Bekele-Arcuri, M. F. Matos, and J. S. Trimmer. 1997. Association and colocalization of the Kvβ1 and Kvβ2 β-subunits with Kv1 α-subunits in mammalian brain K⁺ channel complexes. *J. Neurosci.* 17:8246.

24. Garcia-Calvo, M., R. J. Leonard, J. N. Novick, S. P. Stevens, W. Schmalhofer, G. J. Kaczorowski, and M. L. Garcia. 1993. Purification, characterization, and biosynthesis of margatoxin, a component of *Centruroides margaritatus* venom that selectively inhibits voltage-dependent potassium channels. *J. Biol. Chem.* 268:18866.

25. Kalman, K., M. W. Pennington, M. D. Lanigan, A. Nguyen, H. Rauer, V. Mahnir, K. Paschetto, W. R. Kem, S. Grissmer, G. A. Gutman, et al. 1998. ShK-Dap²², a potent Kv1.3-specific immunosuppressive polypeptide. *J. Biol. Chem.* 273:32697.

26. Trimmer, J. S., and K. J. Rhodes. 2004. Localization of voltage-gated ion channels in mammalian brain. *Annu. Rev. Physiol.* 66:477.

27. Soler, C., R. Valdés, J. García-Manteiga, J. Xaus, M. Comalada, F. J. Casado, M. Modolell, B. Nicholson, C. MacLeod, A. Felipe, et al. 2001. Lipopolysaccharide-induced apoptosis of macrophages determines the up-regulation of concentrative nucleoside transporters Cnt1 and Cnt2 through tumor necrosis factor-α-dependent and -independent mechanisms. *J. Biol. Chem.* 276:30043.

28. Vicente, R., M. Coma, S. Busquets, R. Moore-Carrasco, F. J. López-Soriano, J. M. Argilés, and A. Felipe. 2004. The systemic inflammatory response is involved in the regulation of K⁺ channel expression in brain via TNF-α-dependent and -independent pathways. *FEBS Lett.* 572:189.

29. Kotecha, S. A., and L. C. Schlichter. 1999. A Kv1.5 to Kv1.3 switch in endogenous hippocampal microglia and a role in proliferation. *J. Neurosci.* 19:10680.

30. Rettig, J., S. H. Heinemann, F. Wunder, C. Lorra, D. N. Parcej, J. O. Dolly, and O. Pongs. 1994. Inactivation properties of voltage-gated K⁺ channels altered by presence of β-subunit. *Nature* 369:289.

31. Accili, E. A., J. Kiehn, Q. Yang, Z. Wang, A. M. Brown, and B. A. Wible. 1997. Separable Kvβ subunit domains alter expression and gating of potassium channels. *J. Biol. Chem.* 272:25824.

32. Bähring, R., C. J. Milligan, V. Vardanyan, B. Engeland, B. A. Young, J. Dannenberg, R. Waldschutz, J. P. Edwards, D. Wray, and O. Pongs. 2001. Coupling of voltage-dependent potassium channel inactivation and oxidoreductase active site of Kvβ subunits. *J. Biol. Chem.* 276:22923.

33. Jing, J., D. Chikvashvili, D. Singer-Lahat, W. B. Thornhill, E. Reuveny, and I. Lotan. 1999. Fast inactivation of a brain K⁺ channel composed of Kv1.1 and Kvβ1.1 subunits modulated by G protein β γ subunits. *EMBO J.* 18:1245.

34. Wang, Z., J. Kiehn, Q. Yang, A. M. Brown, and B. A. Wible. 1996. Comparison of binding and block produced by alternatively spliced Kvβ1 subunits. *J. Biol. Chem.* 271:28311.

35. Peri, R., B. A. Wible, and A. M. Brown. 2001. Mutations in the Kvβ 2 binding site for NADPH and their effects on Kv1.4. *J. Biol. Chem.* 276:738.

36. Martel, J., G. Dupuis, P. Deschênes, and M. D. Payet. 1998. The sensitivity of the human Kv1.3 (hKv1.3) lymphocyte K⁺ channel to regulation by PKA and PKC is partially lost in HEK 293 host cells. *J. Membr. Biol.* 161:183.

37. Hajdú, P., Z. Varga, C. Pieri, G. Panyi, and R. Gáspár, Jr. 2003. Cholesterol modifies the gating of Kv1.3 in human T lymphocytes. *Pflugers Arch.* 445:674.

38. Deutsch, C., D. Krause, and S. C. Lee. 1986. Voltage-gated potassium conductance in human T lymphocytes stimulated with phorbol ester. *J. Physiol.* 372:405.

39. England, S. K., V. N. Uebele, J. Kodali, P. B. Bennett, and M. M. Tamkun. 1995. A novel K⁺ channel β-subunit (hKvβ 1.3) is produced via alternative mRNA splicing. *J. Biol. Chem.* 270:28531.

40. England, S. K., V. N. Uebele, H. Shear, J. Kodali, P. B. Bennett, and M. M. Tamkun. 1995. Characterization of a voltage-gated K⁺ channel β subunit expressed in human heart. *Proc. Natl. Acad. Sci. USA* 92:6309.

41. Shi, G., K. Nakahira, S. Hammond, K. J. Rhodes, L. E. Schechter, and J. S. Trimmer. 1996. β subunits promote K⁺ channel surface expression through effects early in biosynthesis. *Neuron* 16:843.

42. Xu, J., and M. Li. 1997. Kvβ2 inhibits the Kvβ1-mediated inactivation of K⁺ channels in transfected mammalian cells. *J. Biol. Chem.* 272:11728.

43. Xu, J., W. Yu, J. M. Wright, R. W. Raab, and M. Li. 1998. Distinct functional stoichiometry of potassium channel β subunits. *Proc. Natl. Acad. Sci. USA* 95:1846.

44. Gulbis, J. M., S. Mann, and R. MacKinnon. 1999. Structure of a voltage-dependent K⁺ channel β subunit. *Cell* 97:943.

45. Hamilton, J. A. 1997. CSF-I signal transduction: what is of functional significance? *Immunol. Today* 18:313.

46. Valledor, A. F., J. Xaus, M. Comalada, C. Soler, and A. Celada. 2000. Protein kinase Cε is required for the induction of mitogen-activated protein kinase phosphatase-1 in lipopolysaccharide-stimulated macrophages. *J. Immunol.* 164:29.

47. Comalada, M., J. Xaus, A. F. Valledor, C. Lopez-Lopez, D. J. Pennington, and A. Celada. 2003. PKCε is involved in JNK activation that mediates LPS-induced TNF-α, which induces apoptosis in macrophages. *Am. J. Physiol.* 285:C1235.

48. Kwak, Y. G., R. A. Navarro-Polanco, T. Grobaski, D. J. Gallagher, and M. M. Tamkun. 1999. Phosphorylation is required for alteration of Kv1.5 K⁺ channel function by the Kvβ1.3 subunit. *J. Biol. Chem.* 274:25355.

49. Kwak, Y. G., N. Hu, J. Wei, A. L. George, Jr., T. D. Grobaski, M. M. Tamkun, and K. T. Murray. 1999. Protein kinase A phosphorylation alters Kvβ1.3 subunit-mediated inactivation of the Kv1.5 potassium channel. *J. Biol. Chem.* 274:13928.

50. Xaus, J., M. Comalada, A. F. Valledor, J. Lloberas, F. J. López-Soriano, J. M. Argilés, C. Bogdan, and A. Celada. 2000. LPS induces apoptosis in macrophages mostly through the autocrine production of TNF-α. *Blood* 95:3823.

51. Nussler, A., J. C. Drapier, L. Renia, S. Pied, F. Miltgen, M. Gentilini, and D. Mazier. 1991. L-Arginine-dependent destruction of intrahepatic malaria parasites in response to tumor necrosis factor and/or interleukin 6 stimulation. *Eur. J. Immunol.* 21:227.

52. Victor, V. M., and M. De la Fuente. 2002. N-acetylcysteine improves in vitro the function of macrophages from mice with endotoxin-induced oxidative stress. *Free Radical Res.* 36:33.

Association of Kv1.5 to Kv1.3 contributes to the major voltage dependent K$^+$ channel in macrophages

Summary

Voltage-dependent K$^+$ (Kv) currents in macrophages are mainly mediated by Kv1.3 but electrophysiological recordings indicate that the channel composition could be more complex than that described in T-cells. K$^+$ currents in bone marrow-derived and Raw-264.7 macrophages are sensitive to Kv1.3 blockers but, contrarily to T-lymphocytes, macrophages expressed Kv1.5. *Shaker* subunits (Kv1) form homo- and heterotetrameric complexes, leading to biophysically and pharmacologically distinct channels. We aimed whether Kv1.5 has a role in Kv currents in macrophages. Thresholds for activation, half-activation voltages and pharmacology indicate that K$^+$ currents could be accounted for by different Kv complexes in macrophages. Furthermore Kv1.3 and Kv1.5 co-localize at the membrane. Co-expression of Kv1.3 and Kv1.5 in HEK-293 cells showed that the presence of Kv1.5 leads to a positive shift in K$^+$ current half-activation voltages. Similarly to Kv1.3, Kv1.3/Kv1.5 heteromers are sensitive to r-Margatoxin in HEK-293 cells. In addition, both proteins co-immunoprecipitate and co-localize and FRET studies further demonstrated that Kv1.5 and Kv1.3 form heterotetramers. Electrophysiological and pharmacological studies of different ratios of Kv1.3 and Kv1.5 co-expressed in *Xenopus* oocytes demonstrate that different Kv1.3/Kv1.5 hybrids might be responsible for K$^+$ currents in macrophages. TNF-B-induced activation of macrophages increased Kv1.3 with no changes in Kv.1.5, in agreement with a hyperpolarized shift in the half-activation voltage. Our results support that Kv1.5 co-associates with Kv1.3, generating functional heterotetramers in macrophages. In response to different physiological stimuli, changes in the oligomeric composition of functional Kv channels could give rise to different biophysical properties, which would lead to the precise immune response.

Introduction

Voltage-dependent potassium channels (Kv) play a crucial role in excitable cells by determining resting membrane potential and controlling action potentials (1). In addition, they are also involved in the activation and proliferation of leukocytes (2). Functional Kv complexes are formed by four transmembrane B subunits and up to four cytoplasmic B subunits (3). The mammalian *Shaker* family (Kv1) contains at least eight different genes (Kv1.1-Kv1.8), coding for B subunits, that can form functional homo- and heterotetrameric complexes (4,5). Thus, Kv1 proteins can assemble promiscuously, yielding a wide variety of biophysically and pharmacologically distinct channels.

However, while a number of studies have demonstrated that specific Kv heteromeric complexes could predominate in nerve and muscle, many other possible combinations are not detected (6,7). Therefore, this mechanism of channel assembly may underlie some of the functional diversity of potassium currents found in the brain and the cardiovascular system.

Bone marrow derived macrophages are cells fully differentiated, and proliferate and activate separately. These cells play a key role at inflammatory loci, where they

115

arrive 24 to 48 hours after lesion and remain until inflammation disappears. However, the persistence of macrophages at inflammatory loci is associated with the pathogenesis of a wide range of inflammatory diseases. Kv are tightly regulated during proliferation and activation in macrophages and their functional activity is important for cellular responses (8). Proliferation and activation trigger an induction of the outward K^+ current that is under transcriptional and translational control. Several lines of evidence indicate that posttranslational events are involved in Kv regulation. In this context, assigning specific K^+ channel clones to native currents is difficult, since this complexity is further enhanced by heteromultimeric assembly of different Kv subunits. Lymphocytes express several voltage-dependent K^+ currents (*n, n'* and *l*-type channels). While Kv1.3, the major Kv channel in leukocytes, is associated with the *n*-type channel and Kv3.1 accounts for the *l*-type, the proteins responsible for the *n'*-type are unknown (2). The electrophysiological properties of Kv1.3 expressed in T-cells and heterologous expression systems are significantly different from those described in macrophages (9). Furthermore, contrary to T-lymphocytes, brain and bone marrow macrophages also express Kv1.5 (8,10). Kv1.3 and Kv1.5 differ in their biophysical and pharmacological properties and show differential regulation in a number different cell types (8,11,12,13). Thus, different K^+

channel subunit composition could lead to specific alteration of cellular excitability, thus determining the specific cellular response.

The aim of the present work is to explore whether Kv1.5 play a role in the major voltage dependent K^+ current generating functional heterotetrameric Kv1.3/Kv1.5 complexes in macrophages. Our results suggest that Kv1.5 co-associates to Kv1.3 generating functional heterotetrameric channels in macrophages. Upon different physiological stimuli, changes in the oligomeric composition of functional Kv could be crucial in intracellular signals determining the specific macrophage response.

Experimental Procedures

Animals and Cell Culture. Bone marrow derived (BMDM) and Raw 264.7 macrophages, human embryonic kidney 293 (HEK-293) cells, EL-4 T-cell line and *Xenopus laevis* oocytes were used. BMDM from 6- to 10-wk-old either BALB/c mice (Charles River laboratories) were isolated and cultured as described elsewhere (8). Briefly, animals were killed by cervical dislocation, and both femurs were dissected removing adherent tissue. The ends of bones were cut off and the marrow tissue was flushed by irrigation with medium. The marrow plugs were passed through a 25-gauge needle for dispersion. The cells were cultured in plastic dishes (150 mm) in DMEM containing 20% FBS and 30% L-

cell conditioned media as a source of Macrophage-Colony Stimulating Factor. Macrophages were obtained as a homogeneous population of adherent cells after 7 days of culture and maintained at 37ºC in a humidified 5% CO_2 atmosphere. Raw 264.7 macrophages, EL-4 and HEK-293 cells were cultured in DMEM culture media, containing 10% FBS supplemented with 10U/ml penicillin and streptomycin, and 2mM L-glutamine. Cells were grown in 100 mm tissue culture dishes for sample collection and onto non-coated glass cover slips for electrophysiology and confocal imaging. In some experiments, Raw 264.7 cells were incubated with 100ng/ml of recombinant TNF-B (PrepoTech E) during 24 hours. All animal handling was approved by the ethics committee of the University of Barcelona in accordance with EU regulations.

RNA isolation and RT-PCR analysis. Total RNA from tissues (brain, liver) and cell lines was isolated using the Tripure isolation reagent (Roche Diagnostics). Ready-to-Go RT-PCR Beads (Amersham Pharmacia Biotech) were used in a one-step RT-PCR reaction. Total RNA and Kv1.3, and Kv1.5 primers were added to the beads as described (14). Forward (F) and reverse (R) oligonucleotide sequences and accession numbers (AN) were as follows: Kv1.3 (AN: M30441), F:5'-CTCATCTCCATTGTCATCTTCTGA-3' (base pairs: 741-765) and R:5'-TTGAAGTTGGAAACAATCAC-3' (base

pairs: 1459-1440); Kv1.5 (AN: AF302768), F:5'-GGATCACTCCATCACCAG-3'(base pairs: 3003-3020) and R:5'-GGCTTCCTCCTCCTTCCTTG-3' (base pairs: 3337-3320). The RT reaction was initiated by incubating the mixture at 42ºC for 30 min. Once the first-strand cDNA was synthesized, the conditions were set for further PCR: 92ºC for 30 sec, 58ºC for 1 min and 72ºC for 1 min. These settings were applied for 30 cycles.

Protein extracts, Immunoprecipitation and western blot. Cells were washed twice in cold phosphate-buffered saline (PBS) and lysed on ice with lysis solution (1% NP40, 10% glycerol, 50 mmol/L HEPES pH 7.5, 150 mmol/L NaCl) supplemented with 1μg/ml aprotinin, 1μg/ml leupeptin, 86μg/ml iodoacetamide and 1mM phenylmethylsulfonyl fluoride as protease inhibitors. In order to obtain enriched membrane preparations homogenates were centrifuged at 3000 *g* for 10 min and the supernatant was further centrifuged at ~150000 *g* for 1,30 h. The pellet was resuspended in Hepes 30 mM (pH 7.4), and protein content was determined by Bio-Rad Protein Assay (Bio-Rad). Samples were aliquoted and stored at –80ºC.

Crude membrane protein samples (50 μg) were boiled in Laemmli SDS loading buffer and separated on 10% SDS-PAGE. They were transferred to nitrocellulose membranes (Immobilon-P, Millipore) and blocked in 5% dry milk-supplemented 0.1% Tween 20 PBS before immunoreaction.